

Solar cycle indices from the photosphere to the corona: measurements and underlying physics

Ilaria Ermolli · Kiyoto Shibasaki ·
Andrey Tlatov · Lidia van Driel-Gesztelyi

Received: date / Accepted: date

Abstract A variety of indices have been proposed in order to represent the many different observables modulated by the solar cycle. Most of these indices are highly correlated with each other owing to their intrinsic link with the solar magnetism and the dominant eleven year cycle, but their variations may differ in fine details, as well as on short- and long-term trends. In this paper we present an overview of the indices that are often employed to describe the many features of the solar cycle, moving from the ones referring to direct observations of the inner solar atmosphere, the photosphere and chromosphere, to those deriving from measurements of the transition region and solar corona. For each index, we summarize existing measurements **and typical use**, and for those that quantify physical observables, we describe the underlying physics.

Keywords Solar cycle · Solar atmosphere · Solar magnetism

I. Ermolli
INAF Osservatorio Astronomico di Roma, via Frascati 33, 00040 Monte Porzio Catone, Italy
E-mail: ermolli@oaroma.inaf.it

K. Shibasaki
Nobeyama Solar Radio Observatory NAOJ, 462-2 Nobeyama, Minamimaki, Minamisaku,
Nagano 384-1305, Japan
E-mail: shibasaki.kiyoto@nao.ac.jp

A. Tlatov
Kislovodsk Mountain Astronomical Station of the Pulkovo Observatory, Kislovodsk, Russia
E-mail: tlatov@mail.ru

L. van Driel-Gesztelyi
University College London, Mullard Space Science Laboratory, Holmbury St. Mary, Dorking,
Surrey RH5 6NT, UK
LESIA, Observatoire de Paris, CNRS, UPMC, Universit Paris Diderot, Paris, France
Konkoly Observatory of the Hungarian Academy of Sciences, H-1121 Budapest, Hungary
E-mail: Lidia.vanDriel@obsppm.fr

1 Introduction

The solar cycle, i.e. the cyclic regeneration of the appearance of the Sun that occurs with a dominant eleven year period, originates below the visible surface of the Sun. In a thin shear layer at the bottom of the convection zone, the turbulent convection operates, jointly with rotational shear, global circulations and boundary layers, to produce magnetic fields by dynamo processes. These fields thread their way to the solar surface, where they manifest themselves with the rich variety of features observed on the solar atmosphere. The evolution of these features constitutes the solar activity cycle. Most recent models and observations of the solar cycle are reviewed e.g. by Charbonneau (2010), Charbonneau et al. (2014) and Hathaway (2010).

Cyclic variability has been detected in cool stars like the Sun (Hall 2008; Oláh et al. 2009; Reiners 2012; Chaplin and Basu 2014). However, the Sun is the only star where its activity cycle has been studied in detail. Indeed, the Sun has been monitored systematically since the advent of the telescope in the early 17th century.

Early observations have shown that the Sun has sunspots that move on the solar disk due to the **solar differential rotation** (e.g. Galilei 1613; Scheiner 1626–1630). More than two centuries later the number of sunspots was recognized to have a cyclic variation (Schwabe 1843). Then, it was found that the latitudinal distribution of sunspots and its progression over the sunspot cycle follow a “butterfly diagram” (Maunder 1904). **This diagram is now a representative image of the solar cycle.**

Sunspots were give a foundation of physics in the early decades of 20th century, when they were demonstrated to be the seat of strong magnetic fields (Hale 1908). The magnetic laws of the solar cycle became apparent (Hale et al. 1919; Hale 1924; Hale and Nicholson 1925) once the measurements of magnetic fields in sunspots were extended over more than a single sunspot cycle. Sunspot and later polar magnetic field measurements also revealed the reversal of the global magnetic field of the Sun with the period of 22 years, the solar (or sunspot) cycle being half of the magnetic cycle (Babcock 1959).

Sunspots are the most commonly known, but only one, among the many manifestations of the solar magnetic fields, which structure the Sun’s atmosphere and make it variable (e.g. Solanki et al. 2006; Stenflo 2008, 2013). This is shown in Figure 1, which presents three simultaneous views of the Sun at different heights in the solar atmosphere, from the photosphere to the corona, and the contemporaneous measurements of the magnetic field in the photosphere.

The cyclic variability of sunspots was found to affect all the manifestations of the solar magnetism on the Sun’s atmosphere, including striking eruptive events that are driven by the evolution of magnetic fields at small scales, such as flares, prominences, and coronal mass ejections. The number of these events follows the rise and decay of the solar cycle (e.g. Hudson et al. 2014a, and references therein). **The solar cycle also characterizes the radiant behavior**

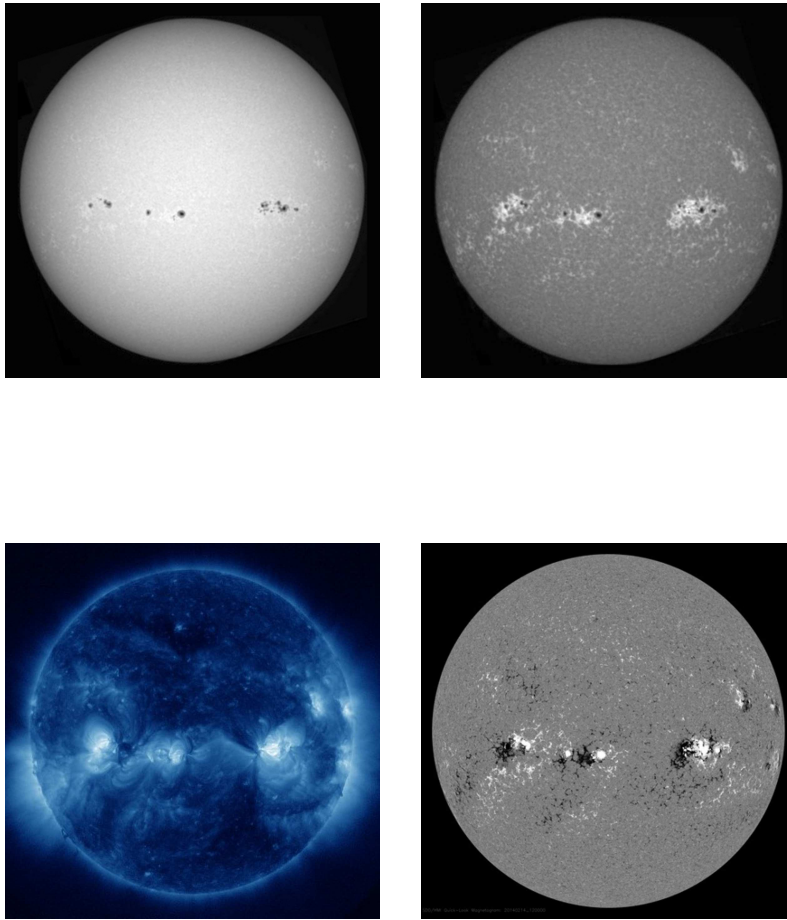


Fig. 1 Simultaneous views of the Sun at different heights in the solar atmosphere and measurements of magnetic field in the photosphere. Top panels: The photosphere (left) observed in the light of the wavelength 430 nm of the CH G-band on 14 February 2014, showing sunspots and faculae, the latter being apparent as bright regions mostly near the disk limb. The chromosphere (right) observed at the Ca II K line radiation at wavelength 393 nm showing the enhanced chromospheric emission from the photospheric magnetic regions. The chromospheric extensions of the faculae (the so-called “plages”) are readily visible across the whole disk (images courtesy INAF Osservatorio Astronomico di Roma). Bottom panels: The contemporaneous views of active regions and full-disk solar corona (left) observed at wavelength 33.5 nm of the Fe XVI line and magnetogram (right) measurement of the line-of-sight (LOS) magnetic field (images courtesy SDO/AIA and SDO/HMI).

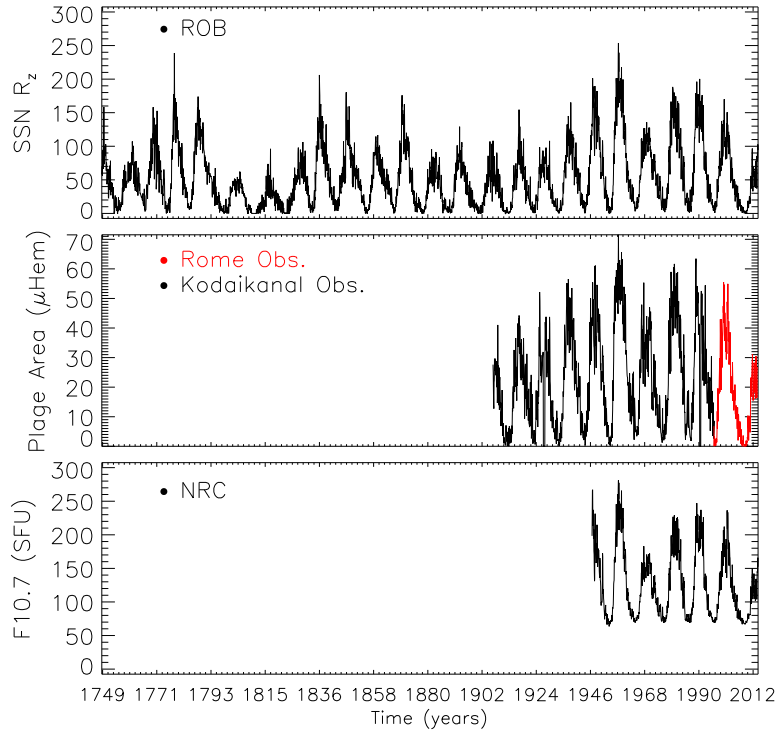


Fig. 2 Comparison of three indices of solar cycle. Monthly averaged values of the international sunspot number (top panel) from the **ROB-SILSO** archive (January 1749 – March 2014), the Ca II K plage area (middle panel) from observations carried out at the Kodaikanal (black symbols) and Rome (red symbols) observatories (February 1907 – August 1996 and May 1996 – November 2013, respectively), and the F10.7 index (bottom panel) from the NRC series (February 1947 – March 2014). **The plage area is expressed in millionths of a solar hemisphere (μHem), whereas the F10.7 index values are given using the Solar Flux Units (SFU, $10^{22} \text{ W m}^{-2} \text{ Hz}^{-1}$).** All indices show common features (eleven year cycle, long-term trends), but each index also reflects a specific aspect of solar activity.

of the Sun (Willson et al. 1981; Hudson et al. 1982; Domingo et al. 2009) and there is growing evidence that changes in solar irradiance affect the Earth's middle and lower atmosphere (e.g. Ermolli et al. 2013; Solanki et al. 2013, and references therein). Besides, as solar magnetic fields are dispersed into the heliosphere with the solar wind, the solar cycle modulates the particulate and magnetic fluxes in the heliosphere, by determining the interplanetary conditions and imposing electromagnetic forces that affect the planetary atmospheres, including the Earth's atmosphere (Cranmer 2009). **Indeed, the large scale structure and dynamics of the magnetic field in the heliosphere is governed by the solar wind flow, which has its origin in the magnetic structure of the solar corona driven by the emergence of magnetic flux (e.g. Schmieder et al. 2014, and references therein), plasma motions in the photosphere and transient solar eruptions in the corona. Most of the flux emerged in the photosphere forms chromospheric or coronal loops that do not contribute to the heliospheric magnetic field carried by the solar wind, but a fraction of flux extends out to form the heliospheric magnetic field, whose variations are an important source of geomagnetic activity (e.g. Pulkkinen 2007; Pulkkinen et al. 2007).** Interplanetary transients and geomagnetic disturbances are found to be related to the changing magnetic fields on the solar surface (Lockwood 2013; Owens and Forsyth 2013; Wang 2014), which indirectly modulate also the flux of high-energy galactic cosmic rays entering the solar system from elsewhere in the galaxy (e.g. Usoskin 2013). Besides, as ^{14}C and ^{10}Be radioisotopes are produced in the Earth's stratosphere by the impact of galactic cosmic rays on ^{14}N and ^{16}O , the solar cycle modulation of the cosmic ray flux also leads to solar cycle related variations in the abundances of ^{14}C (Stuiver and Quay 1980) and ^{10}Be (Beer et al. 1990) in the Earth's atmosphere. **Records of geomagnetic and cosmogenic isotope abundance variations can then be used to infer the near-Earth solar wind conditions and the magnetic field structure and intensity (Lockwood 2013; Svalgaard 2014; Hudson et al. 2014b). Lockwood (2013) gives detailed description of a large number of geomagnetic indices linked to the amount of heliospheric open flux, allowing its reconstruction of from historic geomagnetic activity observations.**

A variety of indices have been proposed in order to represent the many different observables modulated by the solar cycle. Most of these indices are highly correlated with each other as they are intrinsically inter-linked through solar magnetism and its dominant eleven year cycle. **However, they may differ in many features, as well as on short- and long-term trends. This is shown in Figure 2, which presents** the time series of monthly averaged values of three solar cycle indices discussed in the following. All measurements show the eleven year solar cycle, a long-term trend with increasing values in time from 1900 to 1960 and then a reduced solar activity. Apart from these common features, these indices also show clear differences, in particular during the solar minima and on the long-term trends. This is because the

compared indices are related in various ways to different aspects of magnetic processes taking place on the Sun.

We here give an overview of the indices that are often employed to represent solar cycle properties, moving from the ones resulting from direct observations of the inner solar atmosphere, the photosphere (Sect. 2) and chromosphere (Sect. 3), to those deriving from measurements of the transition region and solar corona (Sect. 4). For each index, we summarize existing measurements and typical use, and for those that quantify a directly-measurable value of a physical observable, we describe the underlying physics, before our conclusion are given (Sect. 5). The indices discussed in this paper derive only from observations of the solar atmosphere. Most of these observations have been obtained with ground-based instruments over many decades. A review of the indices that quantify effects caused by the solar magnetism on the heliospheric and terrestrial environments, mostly due to the varying properties of the solar-wind and interplanetary magnetic field, can be found in this volume, e.g., in Usoskin et al. (2014) and Svalgaard (2014), respectively. The solar cycle variation in the total and spectral solar irradiance is reviewed in this volume by Yeo et al. (2014).

2 Indices from observations of the photosphere

Since the advent of the telescope, **sunspots** have been monitored regularly by amateur astronomers and at many observatories. Several indices have been defined from the observed sunspots, **e.g. the international (earlier, Zürich or Wolf) sunspot numbers, the group sunspot numbers, and the sunspot areas. The time series of these indices, which are shown in Figure 3 and further discussed below, are used mainly as proxies of solar activity and as tracers of the dynamo processes responsible for the build-up of large scale magnetic fields into the solar atmosphere.**

Apart from sunspots, faculae¹ are the next obvious feature on the solar disk. They have been known since telescopes have been pointed at the Sun. Observations show their magnetic nature. **They represent magnetic field dispersed from strong magnetic field concentrations in sunspots. Their origin leads facular properties to vary with the sunspot cycle.**

Regular measurements of the magnetic field strength in sunspot and faculae have been carried out in addition to photometric observations since the advent of magnetographs. These measurements have been employed to produce line-of-sight (LOS), or radial, or vectorial estimates of the photospheric magnetic field in physical units, and to obtain some direct and indirect measurements of the magnetic field properties.

¹ Faculae is the name given to brightenings seen in photospheric radiation mainly near the solar limb and in the general vicinity of sunspots. Find more information in e.g. Solanki and Krivova (2009).

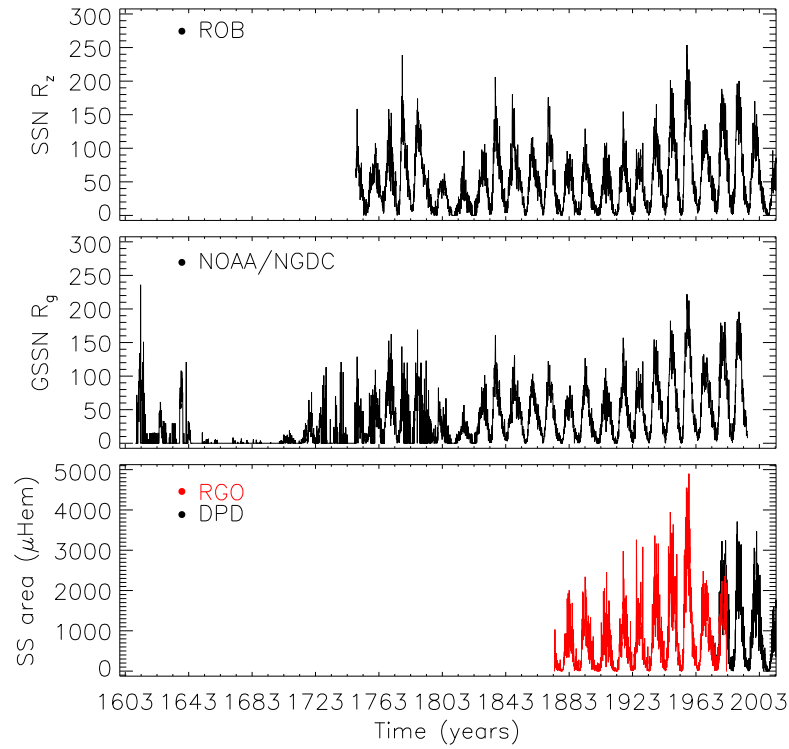


Fig. 3 Comparison of sunspot indices. Monthly averaged values of the international sunspot number (top panel) from the **ROB-SILSO** archive (January 1749 – March 2014), group sunspot number (middle panel) from the NOAA/NGDC archive (February 1610 – December 1995) and sunspot area (bottom panel) from the RGO (red symbols) and DPD (black symbols) series (January 1874 – December 1982 and January 1974 – April 2014, respectively). **The sunspot area is expressed in millionths of a solar hemisphere (μHem).**

2.1 Sunspot number

The sunspot number indicates a weighted estimate of individual sunspots and sunspot groups derived from visual inspection of the solar photosphere in white-light² integrated radiation. The sunspot number was introduced in the middle of the 19th century by Rudolf Wolf, who also started the program of synoptic measurements carried out at the Zürich Observatory that now constitutes the so-called Zürich (or Wolf) sunspot number series. **This measurement series covers the period 1849–1981, but it was extended for several solar cycles backwards by using data available from earlier observations.**

In this series, the sunspot number R_z is defined as:

$$R_z = k(10G + N), \quad (1)$$

where G is the number of sunspot groups, N is the number of individual sunspots in all groups visible on the solar disk and k **denotes a correction factor that compensates for differences in observational techniques and instruments used by the observers.**

The Zürich sunspot number series is based on observations carried out by a single astronomer for each day, by using almost the same technique for the whole period, but an offset due to the changes of the weighting procedure introduced in 1945–1946 and other corrections applied for earlier data. However, it is known that data gaps were filled with interpolation between available measurements without note on the series, by leading to possible errors and inhomogeneities in the data. Besides, the single observers have changed in time, as well as also observatory instruments and practices. **These changes raise** questions about the accuracy and integrity of the sunspot number data series available to date. We omit discussion of this important aspect of the sunspot data and refer the reader to the review in this volume by Clette et al. (2014) for further information.

The Zürich sunspot number data set is available online at e.g. the archive of the National Oceanic and Atmospheric Administrations National Geophysical Data Center (NOAA/NGDC)³.

Since the termination of the sunspot observations at the Zürich Observatory the sunspot number series has been routinely updated as the International Sunspot Number (ISN) by the World Data Center for the production, preservation and dissemination of the international sunspot number (SILSO, Sunpot Index and Long-term Solar Observation⁴) at the Royal Observatory of Belgium (ROB, Clette et al. 2007). The ISN series is computed using the same definition as employed for the Zürich series, but it represents the weighted average of sunspot numbers determined by several approved observers from

² The term white-light indicates the sum of all visible wavelengths of solar radiation from 400 to 700 nm, so that all colors are blended to appear white to the eye.

³ <http://www.ngdc.noaa.gov/stp/solar/ssndata.html>

⁴ <http://www.sidc.be/silso>

more than 30 countries instead of that by a single observer. It is worth noting that sunspot numbers provided by individual stations, e.g. the Zürich series, are often 20 to 50% higher than the ISN value, due to a multiplicative factor introduced to reduce results of modern observations to the scale of the original series started by Rudolf Wolf. Find information on the survey and merging of sunspot catalogs in e.g. Lefevre and Clette (2014). The ISN data are available online at the **ROB-SILSO** web site⁵.

In addition to the data presented above there are series of hemispheric sunspot numbers that account for spots only in the Northern and Southern solar hemispheres. **These series have been used to study e.g. the North-South asymmetry of solar activity (e.g. Temmer et al. 2002, 2006; Virtanen and Mursula 2014; Norton and Charbonneau 2014).** The data are available at e.g. the **ROB-SILSO** web page.

2.2 Group sunspot number

Analysis of the Zürich series and of early sunspot data by Douglas Hoyt and Kenneth Schatten lead to the definition of the group sunspot number and creation of a time series of this index based on all the available archival sunspot records since 1610 (Hoyt and Schatten 1996, 1998a,b).

In this series, the group sunspot number R_g is defined as:

$$R_g = \frac{12.08}{n} \sum_i k'_i G_i, \quad (2)$$

where G_i is the number of sunspot groups recorded by the i -th observer, k' is the observers individual correction factor, n is the number of observers for the particular day, and 12.08 is a normalization number scaling the group sunspot number to sunspot number values for the period of 1874–1976. The group sunspot number is more robust than the sunspot number since **it is based on the easier identification of sunspot groups than of individual sunspots. Besides, it does not include the number of individual sunspots that is strongly influenced by instrumental and observational conditions. Therefore, although the group sunspot number series suffers some uncertainties (see, e.g. Vaquero et al. 2012; Leussu et al. 2013),** it is more reliable and homogeneous than the Zürich series. The two series are nearly identical after the 1880s (e.g. Hathaway and Wilson 2004).

The group sunspot number data set is available online at the NOAA/NGDC archive⁶.

In the recent years, the recovery, digitization, and analysis of archived sunspot drawings regularly produced by several observers from early decades of 17th to late 19th centuries (e.g. Arlt et al. 2013; Vaquero and Trigo 2014; Arlt

⁵ <http://www.sidc.be/silso/datafiles>

⁶ <http://www.ngdc.noaa.gov/stp/solar/ssndata.html>

and Weiss 2014, and references therein) has allowed improvement of earlier uncertain sunspot data and extension for several cycles back in time of the butterfly diagram.

2.3 Sunspot area

Sunspot areas and positions were diligently recorded by the Royal Observatory in Greenwich (RGO) from 1874 to 1976, **by using** measurements from photographic plates obtained at the RGO and other observatories (Cape Town, South Africa, Kodaikanal, India, and Mauritius). Both umbral areas and whole spot areas were measured and corrected for apparent distortion due to the curvature of the solar surface (Willis et al. 2013b,a). Sunspot areas are given in units of millionths of a solar hemisphere.

Since 1976 the RGO measurements have been continued in the Debrecen Photoheliographic Data (DPD) sunspot catalogue **that is compiled by the Debrecen Heliophysical Observatory, as commissioned by the International Astronomical Union**. The DPD catalogue includes the heliographic positions and the areas of the sunspots on the full-disk white-light images obtained at the Debrecen and Gyula observatories, as well as from other observatories. The DPD sunspot data **are available online⁷ together with** images of sunspot groups, scans of full-disk white-light observations, and magnetic observations. Moreover, **the US Air Force also started compiling sunspot data from the Solar Optical Observing Network of telescopes (USAF/SOON)⁸ since RGO ceased its program**. Measurements of sunspot area are also available from a number of solar observatories around the world e.g. Catania (1978 – present), Kislovodsk (1954 – present), Kodaikanal (1906 – present), Mt. Wilson (1917 – 1985), Rome (1958 – present), and Yunnan (1981 – present).

The data recorded at the RGO and the other observatories listed above are available at e.g. the NOAA/NGDC archive⁹. **This archive includes** some fragmentary data of sunspot areas obtained for earlier periods from solar drawings (e.g. Lepshokov et al. 2012; Arlt et al. 2013; Vaquero and Trigo 2014).

Sunspot areas are considered to be a more physical characterisation of the solar cycle than sunspot or group numbers, due to the linear relation between sunspot area and total magnetic flux of the sunspot (see e.g. Kiess et al. 2014, and references therein, and see Preminger and Walton (2007) for the underlying cause of non-linearities). Besides, sunspot area data have the additional information on the disc position of the observed features with respect to sunspot number series. For example, Figure 8 of Hathaway (2010) shows the butterfly diagram of the daily sunspot area values as a function of latitude and time from 1874 to 2010 from the RGO and USAF archives.

⁷ <http://fenyi.solarobs.unideb.hu/DPD/index.html>

⁸ <http://www.ngdc.noaa.gov/stp/solar/sunspotregionsdata.html>

⁹ <http://www.ngdc.noaa.gov/stp/solar/sunspotregionsdata.html>

A number of studies have attempted to inter-calibrate the sunspot area measurements available from the various observatories. **The data** were found to be not uniform across the various sets and even within a given set (e.g. Baranyi et al. 2001; Balmaceda et al. 2009; Baranyi et al. 2013, and references therein). For example, the values reported by USAF/SOON series resulted to be significantly smaller than those from RGO measurements (Balmaceda et al. 2009). Li et al. (e.g. 2009) found that the time series of area values corrected for foreshortening on the solar disk and the ISN values are highly correlated, with a high level of phase synchronization between the compared indices in their low-frequency components (7-12 years), and a noisy behavior with strong phase mixing in the high-frequency domain, mainly around the minimum and maximum times of a cycle.

Sunspot area measurements are main input data e.g. to models of total magnetic flux and solar irradiance variations (e.g. Preminger and Walton 2006, 2007; Pagaran et al. 2009a; Krivova et al. 2010, and references therein).

2.4 Magnetic field measurements

Magnetograms are measurements of the net magnetic field strength averaged over the resolution element of the observation and polarity at a given height in the solar atmosphere. The instruments employed to produce these data rely on a variety of techniques applied to measure the polarization of light at various wavelength positions within a solar spectral line. Circular polarization in the opposite sense on either side of a magnetically sensitive spectral line gives a measure of the longitudinal component of the magnetic field vector. Linear polarization provides information on the strength and direction of the magnetic field transverse to the LOS. These measurements have been employed to produce LOS, or radial, or vectorial estimates of the observed magnetic flux density in physical units (either Tesla or Gauss, by using SI or cgs units, respectively).

Full-disk solar magnetograms have been recorded on a daily basis, starting at the Mt Wilson Observatory ¹⁰ in the late 1950s, then with higher spatial resolution at the National Solar Observatory (NSO) Kitt Peak since the early 1970s, with the Kitt Peak Vacuum Telescope (KPVT, 1974 – 2003)¹¹ and since 2003 with the Synoptic Optical Long-term Investigations of the Sun (SOLIS) vector-spectromagnetograph (VSM, 2003 – present)¹², at the Wilcox Solar Observatory (WSO, 1975 – present)¹³, and more recently by instruments of the Global Oscillations Network Group (GONG, 2006 – present) ¹⁴. The measurements have been also performed in space with the SOHO Michelson

¹⁰ <http://obs.astro.ucla.edu/intro.html>

¹¹ <http://diglib.nso.edu/ftp.html>

¹² <http://solis.nso.edu/0/index.html>

¹³ <http://wso.stanford.edu>

¹⁴ <http://gong.nso.edu>

Doppler Imager magnetograph (SOHO/MDI, 1996 – 2011)¹⁵, and presently by SDO Helioseismic and Magnetic Imager (SDO/HMI, 2010 – present)¹⁶. The first KPVT observations are characterized by 4 arcsec resolution and daily cadence, while the latter data obtained with the SDO/HMI are characterized by 1 arcsec resolution and 45 second cadence. Most of the magnetogram time series listed above refer to photospheric observations of the either the LOS or radial photospheric magnetic field strength, but the recent SOLIS observations **that are taken by sampling two spectral lines originating** at photospheric and chromospheric heights. SOLIS and SDO/HMI observations also produce vector magnetic field measurements. For example, the synoptic magnetic field movie linked to Figure 13 of Hathaway (2010) shows a magnificent evolution of the solar magnetism during the last two and half solar cycles using NSO magnetograms between 1980 – 2009.

The results of magnetic field measurements are available at the web page of the various institutes and space missions listed above. An online database at the Pulkovo Observatory¹⁷ contains data of magnetic field measurements obtained since 1957 at a number of observatories of the former Soviet Union.

The field measurements have been stored at the various observatories as are and further processed to produce synoptic charts. These charts show the latitude-longitude distribution of the magnetic field during a complete solar rotation and the butterfly diagram patterns. For example, Figure 1 of Petrie (2013) shows the butterfly diagram obtained from NSO Kitt Peak data, summing up the photospheric radial field distributions derived from the longitudinal photospheric field measurements from 1974 to 2013. **These charts are the main input data to numerical models of e.g. the solar dynamo and of the solar outer atmosphere and inner heliosphere (e.g. Riley et al. 2011).**

The results of the synoptic measurements carried out at the WSO¹⁸, NSO, and other observatories have been also **employed to derive the time series of the monopole, dipole, and higher order coefficients of the spherical harmonics** that decompose the magnetic field observations as a function of the surface latitude and longitude. The multipole coefficients **have been used to study the dominant length scales and symmetries of the observed field (e.g. Petrie 2013)**, as well as to predict the value of the sunspot numbers at the next solar maximum (see e.g. Pesnell 2012). The heliospheric consequences of the solar cycle variation of the Sun's low-order magnetic multipoles are discussed in this volume by e.g. Wang (2014).

Measurements carried out at the Mt Wilson Observatory have been also analyzed to produce proxies of sunspot and plage properties, specifically the **Mount Wilson Sunspot and Magnetic Plage Strength Indices, which**

¹⁵ <http://soi.stanford.edu/data/>

¹⁶ <http://jsoc.stanford.edu>

¹⁷ <http://www.gao.spb.ru/database/mfbase/main.e.html>

¹⁸ <http://wso.stanford.edu>

represent the fractional solar surface covered by magnetic fields exceeding 100 Gauss and between 10 and 100 Gauss, respectively. These indices have been employed e.g. to model solar irradiance variations (Jain and Hasan 2004). Moreover, local helioseismology methods have provided a way to map medium-to-large magnetic regions on the far-side hemisphere of the Sun (Lindsey and Braun 1997; González Hernández et al. 2007). The sound waves that pass through areas of strong magnetic fields experience a phase shift (Braun et al. 1992) that can be estimated with respect to the propagation in a non-magnetized atmosphere. Maps of the difference between the model and the measured phase shift have been derived regularly **during the last decade** from 24 hours of solar surface velocity data obtained by the GONG¹⁹ and SOHO/MDI observations. These maps show the locations of shorter travel times due to change of sound speed in strong magnetic-field regions, whose presence modify the local plasma temperature. SDO/HMI²⁰ is providing data continuation after the decommission of SOHO/MDI. Recent improvements **have turned the far-side maps into a useful space weather forecasting tool** (González Hernández et al. 2014).

A number of studies have attempted to inter-calibrate the LOS or radial magnetograph full-disk measurements from one or more observatories (e.g. Liu et al., 2012, and references therein). Riley et al. (2014) compared maps from several of the observatories listed above to identify consistencies and differences among them. They found that while there is a general qualitative agreement among the maps produced by the various programs, there are also some significant differences. They also computed conversion factors that relate measurements made by one observatory to another using both synoptic map pixel-by-pixel and histogram-equating techniques. **Besides, they explored the relationship between the various data sets over more than a solar cycle, by finding that the conversion factors remain relatively constant for most of the studied series.**

2.5 White-light facular indices

White-light faculae were routinely measured at the RGO from 1874 to 1976, **by producing a record of over 100 years of continuous daily measurements of the position and projected area of these features.** These measurements are available at the NOAA/NGDC archive²¹. Besides, polar faculae, i.e. faculae seen at high latitudes (50–90°) in white-light observations, have been also monitored since late 19th century. Regular observations of these features have been carried out at e.g. the RGO (1880–1954), Mt Wilson (1906–1990), Zürich (1945–1965), National Astronomical Observatory of

¹⁹ <http://farside.nso.edu>

²⁰ http://stereo-ssc.nascom.nasa.gov/beam/beam_farside.shtml

²¹ <http://www.ngdc.noaa.gov/stp/solar/wfaculae.html>

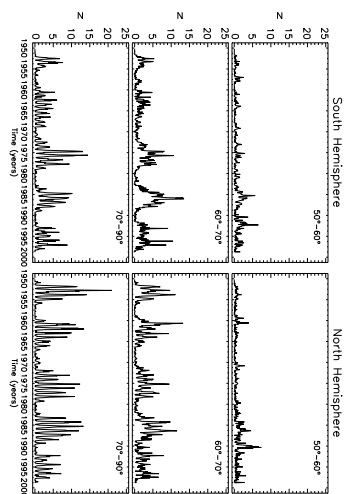


Fig. 4 Monthly averaged value of the number of white-light polar faculae measured from January 1951 to December 1998 at three high-latitude bands: 50–60° (top panels), 60–70° (middle panels), and 70–90° (bottom panels) on the South (left panels) and North (right panels) solar hemispheres. These measurements are from the archive of the National Astronomical Observatory of Japan.

Japan (1951–1997)²², and Kislovodsk (1960 – present)²³ observatories. These observations have shown the counter phase variation of the number of polar faculae with respect to the sunspot cycle. Most recent studies indicate that the phase relationship between numbers of polar faculae and sunspots is both time- and frequency- dependent (Deng et al. 2013). **However, the number of faculae at the poles of the Sun appeared to be well correlated with the LOS component of the polar magnetic field measured at the WSO (Sheeley 2008) and by the SOHO/MDI (Muñoz-Jaramillo et al. 2012), suggesting that the polar faculae number is a good proxy to study the evolution of the polar magnetic field. Observations and models of the solar polar fields are discussed in this volume by e.g. Petrie et al. (2014).**

Figure 4 shows the monthly averaged values of the number of polar faculae at three high-latitude bands on both solar hemispheres from the archive of the National Astronomical Observatory of Japan.

²² <http://solarwww.mtk.nao.ac.jp/solar/faculae/>

²³ http://158.250.29.123:8000/web/P_fac/

3 Indices from observations of the chromosphere

Monitoring programs of full-disk observations in the Ca II K and H $_{\alpha}$ resonance lines have been carried out at various observatories since the start of the 20th century.

The Ca II K line at 393.37 nm is among the strongest and broadest lines in the visible solar spectrum and thus easily accessible to ground-based observations, though in the violet part of the solar spectrum. In solar observations, the core of this line shows an emission reversal, with a central absorption minimum. In standard notation, K₃, K_{2V,2R}, and K_{1V,1R} mark the core, the reversal (emission peaks), and the secondary minima of the doubly reversed profile of the line, in the violet (V) and the red (R) wings of the line, respectively. All these line features occur within a spectral range less than 1 Å wide. They result from a complex formation of the line (Uitenbroek 1989), which originates over atmospheric heights ranging from the temperature minimum photospheric region in the line wing up to the high chromosphere in the core (e.g. Leenaarts et al. 2013).

Observations at the Ca II K have long served as diagnostics of the solar chromosphere (e.g. Rutten 2007, and references therein). They show that the Ca II K line becomes brighter with non-spot magnetic flux. Quantitatively, the line core excess flux density, $\Delta F_{Ca II}$ ($erg\ cm^{-2}s^{-1}$), can be written as:

$$\log \Delta F_{Ca II} = 0.6 \log \langle B \rangle + 4.8, \quad (3)$$

where $\langle B \rangle$ indicates the spatially averaged magnetic flux density in the resolution element of the observation (Schrijver et al. 1989). Therefore, **the Ca II K line emission can be used as a good proxy of the LOS magnetic flux density over the whole solar disk** (e.g. Ermolli et al. 2010, and references therein).

The H $_{\alpha}$ line at 656.28 nm has been also widely employed for studying the solar chromosphere, which was defined as what is seen in this line (Lockyer 1868). The formation of this deep-red line is complicated (Leenaarts et al. 2012) and originates over atmospheric heights ranging from the photosphere in the line wing up to the middle chromosphere in the core (e.g. Leenaarts et al. 2013). Observations at this line show a wealth of magnetically dominated solar features and processes, e.g. flares, filaments, prominences, varying pattern of large-scale magnetic polarity, and the fine structure of magnetic regions. The appearance of these solar features depend on the sensitivity of the H $_{\alpha}$ opacity to the mass density and temperature of the plasma traced by magnetic fields at different heights into the solar atmosphere.

Regular measurements of the solar Mg II h and k resonance lines at 280.27 and 279.55 nm have also been registered from space, as a measure of solar chromospheric variability and good proxies of the solar UV emission (e.g. Dudok de Wit et al. 2009). These lines sample higher layers of the solar chromosphere than the other diagnostics listed above (e.g. Leenaarts et al. 2013, and references therein). **The Mg II core-to wing index has been derived from the Mg II measurements**, by taking the ratio of the

h and k lines of the solar Mg II emission at 280 nm to the background solar continuum near 280 nm (Heath and Schlesinger 1986). The solar Mg II index has been monitored on a daily basis by NOAA spacecraft since 1978. The data are available at the NOAA/NGDC archive²⁴.

The Mg II index has been widely employed e.g. to parameterize the facular and network contribution to short- and long-term solar irradiance variations (Pagaran et al. 2009a; Lean et al. 2011; Fröhlich 2013).

3.1 Ca II K line and plage area indices

Daily full-disk Ca II K observations have been obtained with either spectrographs, Lyot-type, or interference filters at various observatories, e.g. Kodaikanal (1904 – present), Meudon (1909 – present)²⁵, Mt Wilson (1915 – 1985)²⁶, Arcetri (1934 – 1975)²⁷, Big Bear (1942 – 1987), Kislovodsk (1957 – present)²⁸, Rome (1964 – present)²⁹, San Fernando (1984 – present)³⁰, Kanzelhöhe (2010 – present)³¹. The observations at the various sites have been reduced to measure e.g. the position and area of Ca II K plage³² regions, or to derive measurements of the Ca II K line indices described in the following. The data have been **employed to produce synoptic charts of the Ca II K enhanced emission, which reflects the magnetic flux distribution on the solar disk during a complete solar rotation.**

Measurements on modern and historical full-disk Ca II K observations show both cyclic and long-term variations of plage properties (e.g. Ermolli et al. 2009a,b; Foukal et al. 2009; Chapman et al. 2011; Priyal et al. 2014, and references therein). However, similarly to sunspot number series, caution is needed when considering results derived from analysis of long time series of Ca II K full-disk observations, without careful analysis of their problems and intrinsic instrumental variations. In fact, simple visual inspection of the data available at the various archives reveals considerable differences between the images from the various time series, due to different observational and instrumental characteristics. For example, Ermolli et al. (2009a) show that the yearly median values of the plage area measurements derived from the Mt Wilson, Kodaikanal, and Arcetri time series of historical Ca II K observations

²⁴ ftp://ftp.ngdc.noaa.gov/STP/SOLAR_DATA/SOLAR_UV/NOAAMgII.dat

²⁵ <http://bass2000.obspm.fr/>

²⁶ http://www.astro.ucla.edu/~ulrich/MW_SPADP

²⁷ <http://www.oa-roma.inaf.it/solare/index.html>

²⁸ <http://old.solarstation.ru/>

²⁹ <http://www.oaroma.inaf.it/solare/index.html>

³⁰ <http://www.csun.edu/SanFernandoObservatory/>

³¹ <http://cesar.kso.ac.at>

³² Plage is the name given to the brightening seen in chromospheric radiation corresponding to photospheric faculae. In contrast to faculae, plage are seen over the whole disk, in active regions and in the quiet sun, on the network pattern formed at the borders of supergranular cells. Find more information in e.g. Solanki and Krivova (2009).

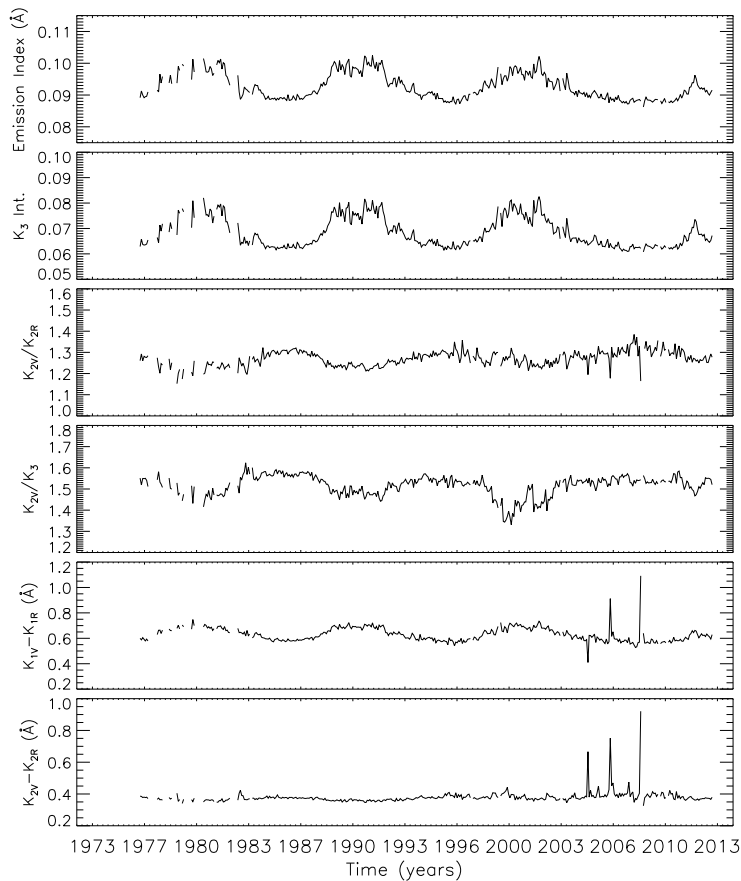


Fig. 5 Time series of monthly averaged values of the Ca II K line parameters measured from November 1976 to April 2014 at the NSO. Details are given in the text.

agree within 40%, with a Pearson correlation coefficient ranging from 0.85 to 0.93. However, the values derived from the three series differ considerably for cycles 15, 17, 19, with a relative difference as high as 140%. Besides, the time series of measured plage area values derived from the three archives show the eleven-year solar cycle variation of the sunspot numbers, but differences at

short time scales are found when comparing sunspot and plage measurements, in particular, subtle but systematic differences around the minima of solar activity, from 1945 to the present. Middle panel of Figure 2 shows the time series of monthly averaged values of the plage area derived from historical and modern Ca II K full-disk observations carried out at the Kodaikanal and Rome observatories, respectively.

Some Ca II K observations listed above **have been also processed to produce time series of indices based on the intensity distribution measured over the solar disk** (e.g. Caccin et al. 1998; Bertello et al. 2010). These indices resulted to be well correlated to the fractional area of the solar disk occupied by plages and network. Besides, **the full-disk Ca II K observations have been employed to study e.g. the onset and end of solar cycles and cycle properties** (e.g. Harvey 1992; Ermolli et al. 2009b). In a recent study Sheeley et al. (2011) computed butterfly diagrams of the longitudinally averaged Ca II K intensity from the Mt Wilson observations for the years 1915-1985. **From analysis of these charts they found that cycle 19 is remarkable for** its broad latitudinal distribution of active regions, its giant poleward surges of flux, and for the emergence of a North-South asymmetry that lasted 10-years. It is worth noting that the CaII K observations exist also for prior sunspot cycles when magnetograms were not available.

Since late 1960s Ca II K line profiles of the Sun were obtained both integrated over the solar disk and at given latitudinal bands at e.g. the NSO in Sacramento Peak and Kitt Peak, and at the Kodaikanal Observatory, by using high resolution spectrographs. For the subsequent decades, these K-line monitoring programs have produced almost daily measurements of several parameters characterizing the Ca II K-line measurements. **The daily observations of the disk integrated Ca II K emission at the NSO Kitt Peak have been obtained with the Integrated Sunlight Spectrometer (ISS) of the SOLIS telescope since 2006.** The ISS monitors the solar emission at nine different wavelength bands regularly³³.

The Ca II K line parameters measured to date include the Ca K emission index, which is defined as the equivalent width of a 1 \AA band centered on the K line core, and various measures of line features (e.g. relative strength of the blue K_2 emission peak with respect to the K_3 intensity, separation of the two emission maxima, separation of the blue and red K_1 minima) and asymmetry (ratio of the blue and red K_2 emission maxima). The data derived from the NSO program are available online³⁴.

Figure 5 shows the time series of monthly averaged values of the Ca II K line parameters measured at the NSO. **A recent analysis of these data by Scargle et al. (2013) indicates that the temporal variation of the measured line parameters consists of five components, including the solar cycle eleven year period, a quasi periodic variation with 100**

³³ <http://solis.nso.edu/iss>

³⁴ http://nsosp.nso.edu/cak_mon/

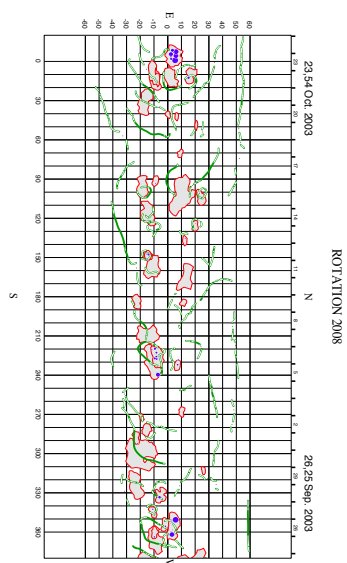


Fig. 6 Synoptic map of solar activity from H_{α} and Ca II K observations obtained at the Meudon Observatory. This map summarizes the properties of solar features observed during their transit across the solar disk from 26 September to 23 October 2003, i.e. for a solar rotation during the last activity maximum. The active regions (sunspots and plage marked with blue and red areas, respectively) and filaments (green areas) observed on the disk are shown at their activity maximum and maximum spread, respectively. The position on the map of the observed features represents the average position of daily baselines.

day period, a broad band stochastic process, a rotational modulation, and random observational errors. Pevtsov et al. (2013) found a weak dependency of intensity in the Ca II K line core measured in the quiet chromosphere with the phase of the solar cycle. This dependency has been attributed to the signature of changes in thermal properties of basal chromosphere with the solar cycle.

3.2 H_{α} filament and prominence data

Daily full-disk H_{α} observations have been obtained with either filters or spectroheliographs at various observatories, e.g. Meudon (1909 – present)³⁵, Arcetri (1927 – 1969), Catania (1906 – present)³⁶, Kanzelhöhe (1973 – present)³⁷, and Big Bear (1982 – present)³⁸, to mention a few. **These observations were taken regularly also to support solar-terrestrial prediction services.**

³⁵ <http://bass2000.obspm.fr/home.php>

³⁶ <http://www.oact.inaf.it>

³⁷ http://cesar.kso.ac.at/synoptic/ha4m_years.php

³⁸ <http://www.bbso.njit.edu/Research/FDHA/>

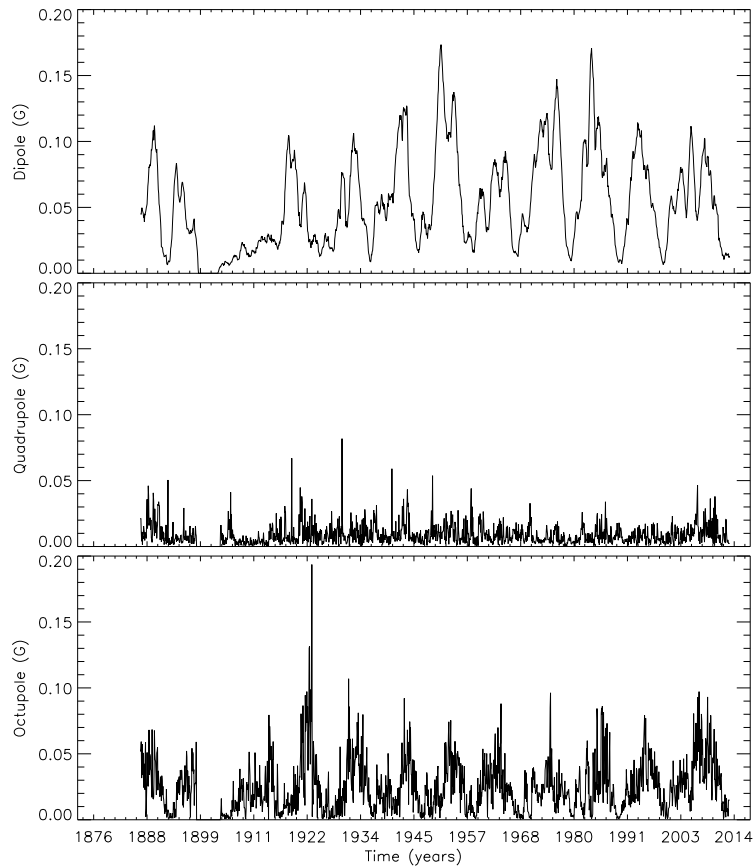


Fig. 7 Monthly averaged values of the dipole, quadrupole, and octupole coefficients of the spherical harmonics that describe the large scale solar magnetic field from the measurements of the filaments, filament channels, and prominences in the H_{α} synoptic charts (January 1887 – December 2013) produced at the Kodaikanal, Meudon, NSO Sacramento Peak, and Kislovodsk observatories.

The data obtained at various observatories have been stored as are and further processed to produce H_α synoptic charts, which incorporates information about evolving features observed in the solar chromosphere at the H_α radiation into a single map for each rotation of the Sun. These charts show e.g. the boundaries separating positive and negative magnetic polarities on the solar surface, and data of the filaments and filament channels. At present, the summary series of these charts cover the period from 1887 up to present (e.g. Vasil'Eva et al. 2002), though earlier data are rather uncertain.

Figure 6 shows the H_α map for a solar rotation at the cycle 23 maximum, from 26 September to 23 October 2003, obtained at the Meudon Observatory. Local H_α and Ca II K observations have been processed (Mouradian 1998) since late 1989 for drawing maps and for computing active region and filament tables. The produced maps show the properties of observed features during their transit across the solar disk. **They display active regions (sunspots and plage) at their activity maximum, i.e. maximum area, and filaments at their maximum spread at the average position of daily baselines.** Other synoptic maps derived from Meudon observations show daily information of filament traces and prominence positions observed on the limb. Besides, there are data of filaments available at the NOAA/NGDC archive³⁹, dating back 1919 and consisting of the position, shape, and life time of the observed features and of their different parts. Other available data include the area of prominences (1957 – present) and filaments (1959 – present) observed at the Kislovodsk station of the Pulkovo Observatory.

Figure 7 shows the coefficient of the spherical harmonic decomposition of the large scale solar magnetic field derived from the field polarity data deduced from the H_α synoptic charts produced at the Kodaikanal, Meudon, NSO Sacramento Peak, and Kislovodsk observatories (see e.g. Makarov and Tlatov 2000; Makarov et al. 2001, for a description of the methods applied). It is noteworthy that the period covered by these charts is comparable to the length of sunspot group series, exceeding the period covered by direct measurements of the large-scale solar magnetic field.

3.3 Flare indices

Flares⁴⁰ are complex multi scale phenomena (Shibata and Magara 2011) that affect different spatial and temporal scales at various heights in the solar atmosphere, from the photosphere to the corona and beyond. Therefore, they are observed at all wavelengths from

³⁹ <http://www.ngdc.noaa.gov/stp/space-weather/solar-data/solar-features/prominences-filaments/filaments/>

⁴⁰ Flare is the name given to a sudden, rapid, and intense brightening observed over the solar disk or at the solar limb, due to a release of magnetic energy (up to 10^{32} erg on the timescale of hours), followed by ejection of solar plasma through the corona into the heliosphere. Find more information e.g. in Benz (2008).

decameter radio waves to gamma-rays at 100 MeV. Occasionally, flares are also seen in white-light photospheric observations (Benz 2008). The X-ray and particle flux emitted during solar flares have been measured regularly since the advent of space missions. However, before the space age, flares were monitored for many years via H_{α} chromospheric observations carried out at many observatories, by visual, photographic, or digital inspection of the solar disk. Although the full effect of the solar cycle on flares is depicted by the measurements of these events recorded at the various wavelength bands, we focus in the following on the flare indices from synoptic observations of the solar chromosphere, because of the remarkable archival data. Indeed, reports of the H_{α} solar flare patrol programs are available from 1938 to present at the NOAA/NGDC archive⁴¹, which holds data for about 80 observing stations. Currently five observatories send their data to the NOAA/NGDC archive on a routine monthly basis. The information stored in these reports include time of beginning-, maximum brightness-, secondary maxima-, and end- of the event, heliographic coordinates of center of gravity of flare at maximum brightness, optical brightness, area of the flaring region at time of maximum brightness. These data are integrated by the X-ray flux of the events as measured from the NOAA satellites SOLRAD (1968 – 1974) and GOES (1975 – present). For GOES X-ray events, the flare is assumed to start when four consecutive 1-minute X-ray flux measurements are above a threshold value, are strictly increasing, and the last value is at least 1.4 times larger than the value measured three minutes earlier. The maximum flux value measured during the flare defines the event size, which is classified by the C-, M-, X- class scale. The event ends when the flux reading returns to half the sum of the flux at maximum plus the flux value at the start of the event.

The flare activity shown by the H_{α} observations has been also described with the “flare index”, whose concept was introduced by Josip Kleczek in early 1950s (Kleczek 1952). **This quantity is defined as the product of the intensity scale of the flare observed in the H_{α} radiation and its duration in minutes. It is assumed to be roughly proportional to the total energy emitted by the flare (e.g. Özgüç et al. 2003, and references therein).** Daily data of the flare index are available at e.g. the NOAA/NGDC archive⁴² and, for solar cycles 20 to 23, also at the site of the Bogazici University⁴³.

Alternative definitions of the flare index exist with respect to that presented above, e.g. the “X-ray flare index” as described e.g. by Criscuoli et al. (2009), based on X-ray flux measurements in the 1-8 Å range of the solar spectrum, and the “Comprehensive Flare Index” computed by Helen Dodson and Ruth Hedeman from observations of the McMath-Hulbert Solar Observatory for the

⁴¹ <http://www.ngdc.noaa.gov/stp/space-weather/solar-data/solar-features/solar-flares/h-alpha/reports/>

⁴² ftp://ftp.ngdc.noaa.gov/STP/SOLAR_DATA/SOLAR_FLARES/INDEX

⁴³ ftp://ftp.koeri.boun.edu.tr/pub/astronomy/flare_index

period from 1955 to 2008. This latter index is based on H_α observations and measurements of the magnitude of the event measured at radio frequencies, as well as of the importance of sudden ionospheric disturbance. The data are available at the NOAA/NGDC archive.

The flare index has been widely employed to single out signatures of the flaring activity in magnetic regions. For example, it has been recently used to test the efficiency of measurements of the topological complexity of the magnetic field concentrations to discriminate between flaring and non-flaring regions (e.g. Georgoulis 2013; Ermolli et al. 2014, and references therein).

4 Indices from observations of the transition region and solar corona

The solar corona has been observed regularly since the advent of the coronagraphs by Bernard Lyot in the early 1930s and the contemporary discovery of the He I 1083 nm infrared line in the solar spectrum by Harold and Horace Babcock (Babcock and Babcock 1934). Since then several coronal quantities have been measured daily. These quantities have been supplemented by the huge data set of imaging observations taken during the space era. These data allow to evince the magnetic structure of the corona that originates the solar wind governing the magnetic field in the heliosphere. Direct measurements of the coronal magnetic field are still scarce to date. However, the coronal field can be modeled by extrapolating the magnetic field observed in the inner solar atmosphere. To this purpose, sunspot data series have been employed as input data to e.g. solar surface transport models coupled with extrapolations of the heliospheric field (e.g. Jiang et al. 2011, and references therein).

The He I line is seen in absorption on the solar disk, but in emission under some special conditions, e.g. during solar flares. The helium absorption is enhanced with respect to the quiet Sun above active regions and H_α filaments (e.g. Brajša et al. 1996), and reduced in coronal holes (CH)⁴⁴. Due to a complex line-formation mechanism (Avrett et al. 1994), the patterns seen in He I 1083 nm line observations are affected by processes in the upper chromosphere, transition region, and low corona. In particular, model calculations show a strong dependence of the line absorption on coronal illumination. Lagg (2007) summarizes the results of magnetic field measurements using the He I line and discusses the potential of this line as a diagnostic of the solar outer atmosphere. Observations at this line have been taken at the NSO Kitt Peak since 1974 on a daily basis.

⁴⁴ Coronal holes are areas where the Sun's corona is darker, and colder, and has lower-density plasma than average. They are associated with rapidly expanding open magnetic fields and the acceleration of the high-speed solar wind. Find more information in e.g. Potgieter (2013).

The solar upper atmosphere also emits radio flux. It consists of free-free emission from quiet sun coronal plasma and gyromagnetic emission from sunspots in active regions (e.g. Shibasaki et al. 2011, and references therein).

The integrated radio flux from the Sun is defined as:

$$F = \frac{2k_B}{\lambda^2} \int T_b d\Omega,$$

where, F , k_B , λ , Ω , are radio flux ($\text{Wm}^{-2}\text{Hz}^{-1}$), the Boltzmann constant, the observing wavelength, and the solid angle of the source respectively. The solar radio flux is measured using the Solar Flux Unit (**SFU**, $10^{-22} \text{Wm}^{-2}\text{Hz}^{-1}$). T_b is called radio brightness temperature and is related to the plasma temperature T as follows:

$$T_b = \int T e^{-\tau} d\tau,$$

where, τ is the optical depth, which is related to the absorption coefficient κ by the relation $d\tau = \kappa dl$, where l is the path length along the line of sight. In the case of thermal free-free emission (collisions of electrons with ions), the absorption coefficient is a function of the plasma density n , the temperature, and the observing wavelength: $\kappa = \xi c^{-2} \lambda^2 n^2 T^{-3/2}$, where ξ is a constant (0.1 in the chromosphere and 0.2 in the corona) and c is the light speed. In an optically thick case ($\tau \gg 1$), the brightness temperature is equal to the plasma temperature and the integrated flux is inversely proportional to square of the measured wavelength. Gyro-resonance is prominent around 3 GHz compared to free-free contribution.

Among the various radio measurements, those pertaining the flux in the wavelength range of 2.8 GHz or 10.7 cm, near the peak of the observed solar radio emission, constitute the longest, most stable and almost uninterrupted record of direct physical data of solar activity available to date. This is because the radio flux measurements are rather insensitive to weather and disturbances in the ionosphere. Historically, this index, which provides the so-called **F10.7 index series**, has been used as an input to ionospheric models as a surrogate for the solar UV output that produces photoionization in the Earth's ionosphere.

4.1 He 1083 nm line observations

Regular observations of the solar disk at the He I line started in late 1930s. These observations were carried out with spectroheliographs until the availability of spectropolarimetric measurements. **The results were mostly employed to investigate the chromospheric topology and dynamics.** After their first detection from space in the late 1960s and early 1970s, most of CH data available to date were later deduced from available He I 1083 nm observations.

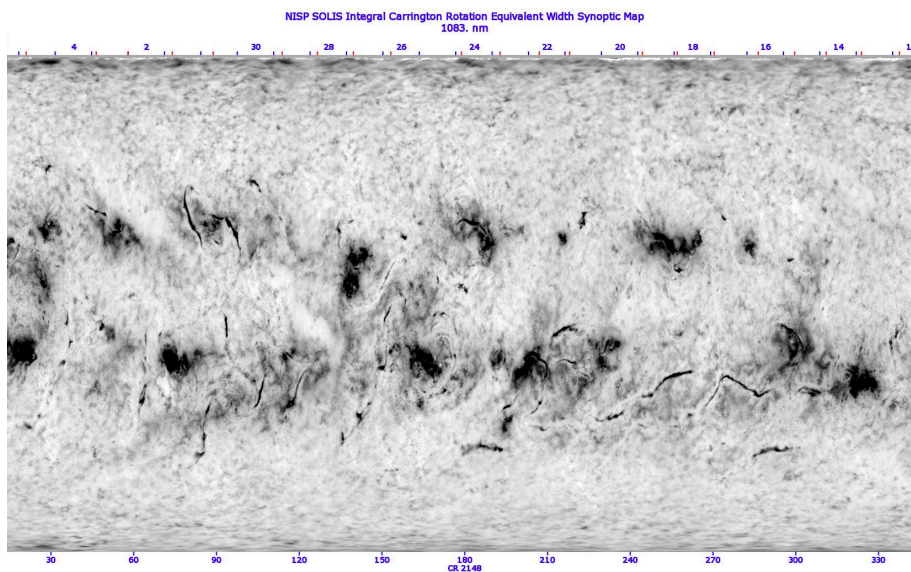


Fig. 8 Map derived from daily full-surface intensity values of the equivalent width as measured from profiles of the spectral line of He I 1083.0 nm. These measurements are from the NSO archive.

Full-disk observations at the He I 1083 nm line have been taken at the NSO Kitt Peak since 1974 (Harvey and Sheeley 1977) on a daily basis, **by using** the KPVT magnetograph. The data were published by the NOAA/NGDC archive⁴⁵ as Helium synoptic charts for each solar rotation or as CH contours plotted on H_{α} synoptic charts. In particular, the latter method was used to determine the polarity of each observed CH, and to identify it over several solar rotations. Magnetograms from NSO Kitt Peak were also used for this purpose. The NSO He I 1083 nm observations have been continued by the SOLIS VSM since 2003. The data obtained consist of full-disk intensity maps representing the equivalent width as measured over the solar disk from profiles of the spectral line of He I 1083 nm.

Figure 8 shows a SOLIS He I synoptic chart for the period from 12 March to 5 April 2014 from the NSO archive. **The data in this archive have been employed to derive information on CH positions. CHs were found at the Sun’s polar regions at solar minimum, and located anywhere on the Sun during solar maximum.** Besides, transient “dark points” in He I 1083 nm observations were found to be associated with small magnetic bipoles. The number of these dark points resulted to vary inversely with the sunspot number (Harvey 1985).

The NSO Kitt Peak He I 1083 nm intensity maps have been used e.g. **by Harvey and Recely (2002) to identify and measure the evolution**

⁴⁵ <http://www.ngdc.noaa.gov>

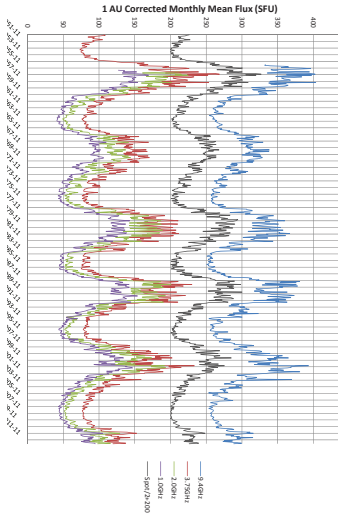


Fig. 9 Monthly averaged values of the radio flux measurements at the 9.4, 3.75, 2, 1 GHz from the NSRO archive (January 1951 – December 2013), corrected for 1 AU distance, superposed to scaled values of the ISN from the **ROB-SILSO** series.

of polar CHs during cycles 22 and 23. They found that polar CHs, which are the largest at cycle minimum, evolve from high-latitude ($\approx 60^\circ$) isolated holes. During the initial 1.2–1.4 years following the polar polarity reversal, the polar CHs develop asymmetric lobes extending to active latitudes **and the area and magnetic flux of the CH increase rapidly.**

4.2 Radio flux data

Synoptic radio measurements have been made at the various observatories since 1945 (Sullivan 1984), by using radio polarimeters, to measure the total coming flux and the circular-polarization degree at various frequencies, and by employing radio heliographs made of many antennas that allow to produce interferometric measurements at various frequencies. The radio emission data available to date include daily values of solar flux density at 30 different frequencies ranging from 0.1 to 15 GHz, and tables of distinctive events. Radio charts of active regions on the Sun have been also derived from the measurements carried out at e.g. the Nancay and Nobeyama observatories.

Radio flux from the Sun consists of three components that can be discriminated by the temporal scale of flux variations (e.g. Tapping 2013, and references therein). The burst component is the flux variation associated with flares on typical time scales from seconds

to hours. It is employed to diagnose high energy particle acceleration and production of thermal plasma associated with flares. The slowly varying (S) component is linked with the evolution of active regions on typical time scales from a day to weeks. The base (B) component is the residual flux after subtraction of the burst and S components. Daily quiet time total flux (daily flux) data consists of S and B components.

As stated above, the time series of the radio flux measured at 2.8 GHz or 10.7 cm, the F10.7 index constitutes the longest record of a physical data of the solar cycle available to present. This index is a measurement of the integrated emission at 10.7 cm wavelength from all sources present on the disk. Daily measurements at local noon of this flux have been made by the National Research Council (NRC) of Canada from 1947 to 1991 in Ottawa and thereafter in Penticton. The flux values (Covington 1969) are expressed in the SFU units introduced above. The data, which are available at the site of the NRC⁴⁶ and NOAA/NGDC archive⁴⁷, include daily F10.7 flux values, monthly averages, and rotational averages computed over a solar rotation. The NOAA/NGDC archive also contain radio measurements obtained at various frequencies e.g. since 1956 at the Astronomical Observatory of the Jagellonian University in Cracow, since 1966 with the USAF Radio Solar Telescope Network operated at various observatories, and from 1962 to 1973 with the Stanford Radio Astronomy Institute telescope.

The second longest record of solar radio measurements is from Japan (Tanaka et al. 1973). Measurement at 3.75 and 9.4 GHz started there in 1951 and 1956, respectively; they were supplemented with measurements at 1.0 and 2.0 GHz in 1957. The measurements were carried out at the Toyokawa observatory till 1994, and thereafter continued at the Nobeyama Solar Radio Observatory (NSRO). Results of these and of the earlier synoptic measurements carried out from 1951 to 1994 are available at the NSRO site⁴⁸.

Figure 9 shows the time series of monthly averaged values of the radio flux measurements from the NSRO archive, superposed to scaled values of the ISN from the ROB-SILSO series. Pearson's correlation coefficients between the radio flux and ISN values are range between ≈ 0.94 and 0.98 .

Additional radio data include those obtained with the Radio Solar Telescope Network started by the Sagamore Hill Solar Radio Observatory in 1966, with stations at Palehua/Kaena, Learmonth, and SanVito, whose observing frequencies are 245, 410, 610, 1415, 2695, 4995, 8800, and 15400 MHz, and by the Kislovodsk station of the Pulkovo Observatory⁴⁹, which started operation in 1960 at wavelengths of 5, 10, 15 GHz (or 2, 3, 5 cm). Besides, since 1996 the Nancay Radio Heliograph (Kerdraon and Delouis 1997) and decametric array

⁴⁶ <http://www.spaceweather.gc.ca/solarflux/sx-5-eng.php>

⁴⁷ http://www.ngdc.noaa.gov/stp/space_weather/solar_data/solar_features/solar_radio/noontime_flux/

⁴⁸ <http://solar.nro.nao.ac.jp/norp/>

⁴⁹ <http://www.gao.spb.ru/english/database/sd/tables.htm>

telescopes ⁵⁰ have been acquiring thousands of interferometric images each day of the solar corona and at very low frequency. The frequencies monitored regularly with these telescopes cover the range 5 – 10 Mhz, 10–100 MHz (from 20 to 75 MHz), higher than 100 MHz (at 164 MHz and 327 MHz). It is worth noting that 1D scans of the Sun were also taken from 1967 to 1996, but the data are not available online. Data from the decametric telescope goes back to 1991 ⁵¹.

The daily F10.7 index was found to be well correlated to sunspot number and area (Denisse 1949). It was then noticed that the radio emission in the range of 3 – 30 cm wavelength, or 10 – 1 GHz frequency range, correlates well with E-layer ionization (Kundu 1970). **Since then the daily F10.7 index has been used as a proxy of solar cycle in models of the Earth’s upper atmosphere.** Recent studies by Tapping and Valdés (2011) and Svalgaard and Hudson (2010) suggested that the relation between sunspot numbers and radio flux has started to deviate from the previous relation since the 23 solar cycle. However, Henney et al. (2012) found that the relation between total magnetic flux on the solar surface and radio flux values does not show any noticeable change in the last cycles. **The results suggest that the F10.7 index is a better proxy of the total magnetic flux on the solar surface than sunspot numbers.**

In a recent study, Dudok de Wit et al. (2014) merged daily observations from the Ottawa/Penticton and Toyokawa/Nobeyama observatories into a single homogeneous data set of the solar flux at wavelengths of 1, 2, 2.8, 3.75, 9.4 GHz (or 30, 15, 10.7, 8 and 3.2 cm), spanning from 1957 to present. They found that most solar proxies, in particular the MgII index, are remarkably well reconstructed by simple linear combination of radio fluxes at various wavelengths. **Their results also indicate that the flux at 1 GHz (or 30 cm) stands out as an excellent proxy of solar cycle and is better suited than the F10.7 index for the modelling the Earth’s thermosphere-ionosphere system.**

4.3 Coronal indices

The intensity of the coronal green radiation from the Fe XIV emission line at 530.3 nm has been observed since 1939 at the Arosa observatory and then recorded from 1947 onwards first at the Climax and Pic du Midi observatories and thereafter at other sites (e.g. at Norikura Observatory⁵² between 1951–2009). The emission of this line can be observed above the entire solar limb during the whole solar cycle, contrary to the emission of other coronal lines, e.g. the Fe X red line at 637.4 nm and the Ca XV yellow line at 569.4 nm, which can be observed only occasionally. The intensity of the green corona depends

⁵⁰ http://secchirh.obspm.fr/nrh_data.php

⁵¹ http://realtime.obs-nancay.fr/dam/data_dam_affiche/

⁵² http://solarwww.mtk.nao.ac.jp/en/db_gline1.html

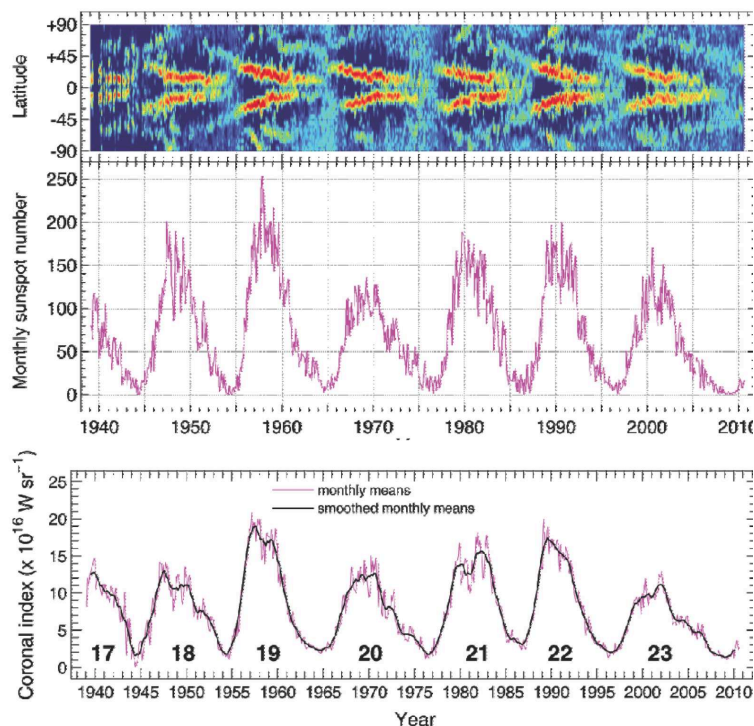


Fig. 10 Time series of the coronal index (CI, bottom panel), the sunspot number (middle), and the Fe XIV 530.3 nm coronal green emission line brightness maxima (top). The CI is computed from the homogeneous dataset (HDS). Panels adapted from Minarovjech et al. (2011).

on both the density and temperature of the plasma in the outer solar atmosphere, and both these quantities are modulated by the local magnetic fields. At present observations of the green corona are made at the Kislovodsk, Lomnický Stit, and Sacramento Peak observatories. The measurements recorded at the various sites differ due to time difference, method of observation, height of the observation above the solar limb, and other parameters. However, the data obtained at these observatories have been processed since 1939 to obtain a physical index of the solar cycle signature on the outer solar atmosphere, the so-called coronal index (CI, e.g. Rybanský et al. 2005, and references therein), and a homogeneous data set (HDS, Minarovjech et al. 2011, see Figure 10).

This data set, which has been obtained by scaling all the available measurements to the photometric scale of the Lomnický Stit observations, is available for the period of 1939 – 2008 at the NOAA/NGDC web page⁵³. Recently, Dorotovič et al. (2014) developed a method to substitute the ground-based ob-

⁵³ <http://www.ngdc.noaa.gov/stp>

servations by space-borne 28.4 nm (Fe XV) observations from the SOHO/EIT data. The dataset, named Modified Homogeneous Dataset (MHDS), extends the HDS beyond 2008. For the period up to 1996, the MHDS is identical with the former HDS. The MHDS is available online⁵⁴ for the 1996 – 2010 period.

The coronal index represents the averaged daily irradiance in the green coronal line emitted in 1 steradian towards the Earth, and it is expressed in (W sr^{-1}) units⁵⁵. **Rušin and Rybansky (2002) analyzed these data to study** the relationship between the intensity of the green corona and strength of photospheric magnetic flux over the period 1976 – 1999, by finding a relation between these indices that allowed them to extend solar surface magnetic fields estimates since 1976 back to 1939, when the green corona began to be observed. A discussion of the coronal index with respect to other solar cycle indices can be found in e.g. Rybanský et al. (2001).

In addition to the integrated flux measurements of the coronal green line emission, other measurements have been also recorded systematically, e.g. the intensity measured around the solar limb, within intervals of 5° , at the coronal lines at 637.4 nm (Fe X), 530.3 nm (Fe XIV) and 569.4 nm (Ca XV). These lines are formed at approximate temperatures of 1, 2 and 3 MK, respectively. These measurements have been also processed to produce full-disk maps from 14 days of measurements projected onto a sphere.

5 Conclusions

For hundreds of years the evolution of the solar features driven by the cyclic variation of the solar magnetic field has been monitored systematically. A variety of indices have been introduced in order to represent the many different results derived from observations of the solar features in time. These indices include values from measurements of physical quantities, e.g. the Ca II K line emission and radio flux, as well as of parameters derived from the observations, the most common being the sunspot numbers. The time series of the sunspot numbers, which constitute one of the longest continuous measurement programs in the history of science, continue to be used as the most common index to describe solar cycle properties. However, additional measurements of more physical quantities modulated by the solar cycle are also available online **to enter the models of e.g. the solar dynamo and of the Earth's climate response to solar variability**, though the time series of the physical quantities are shorter than that of sunspot numbers.

Continuation of the time series of the many indices of solar cycle available to date in the next decades is especially important **since the long-term trends of solar activity have become a topic of great interest and research after the last activity minimum**. Besides, continuous improvement of the accuracy of earlier data and of the whole series, precise long-term data calibration, and extension of the time series back in time, can also lead to

⁵⁴ <http://www.suh.sk>

⁵⁵ Conversion: $1 \times 10^{16} \text{Wsr}^{-1} = 4.5 \times 10^{-7} \text{W m}^{-2} = 1.2 \times \text{photons cm}^{-2}\text{s}^{-1}$.

a better knowledge of the solar cycle and its effects on the whole heliosphere. To this regard, the recovery, digitization, and analysis of historical observations started in recent years, consisting of both full-disk drawings dating back early 17th century and photographic observations taken since 1876 at several observatories, promise to extract from these unexploited data far more detailed information on solar magnetism than just the sunspot number and area records available till recent times.

The availability of long and accurate time series of solar cycle indices has a **large potential impact not only on solar research but also on space weather and space climate studies. Indeed, sunspot number, UV and radio flux series are the key input data to studies of the solar activity impact on the Earth's upper atmosphere and ionosphere (Maruyama 2010), through e.g. multiscale models of traveling ionospheric disturbances (Fedorenko et al. 2013) and data-driven analysis (Kutiev et al. 2013; Scott et al. 2014). Besides, sunspot and plage area, Mg II and F10.7 measurement series enter models of total and spectral solar irradiance variations on long time scales (e.g. Krivova et al. 2010; Lean et al. 2011). These models have been recently employed to study e.g. the influence of spectral solar irradiance variations on stratospheric heating rates (Oberländer et al. 2012; Anet et al. 2013; Thuillier et al. 2014), to estimate the tendency of the Northern Hemisphere temperature for the next decades by using a thermodynamic climate model (Mendoza et al. 2010), to describe the long-term trends in the North Atlantic Oscillation Index (van Loon et al. 2012), and to carry out chemistry climate model experiments of the impact of a time-varying solar cycle and quasi-biennial oscillation forcings on the Earth's atmosphere and the ocean (Petrick et al. 2012; Matthes et al. 2013).**

Finally, the availability of long and accurate time series of solar cycle indices may also improve our ability to predict the future evolution of the solar activity.

Acknowledgements The authors are grateful to the International Space Science Institute, Bern, for the organization of the workshop “The Solar Activity Cycle: Physical Causes and Consequences”, the invitation to contribute to it, and the kind support received to the purpose. The authors thank Fabrizio Giorgi for preparing Figs. 1 to 8. This study received funding from the European Unions Seventh Programme for Research, Technological Development and Demonstration, under the Grant Agreements of the eHEROES (n 284461, www.eheroes.eu), SOLARNET (n 312495, www.solarnet-east.eu), and SOLID (n 313188, projects.pmodwrc.ch/solid/) projects. It was also supported by COST Action ES1005 TOSCA (www.tosca-cost.eu). LvDG's work was supported by the Hungarian Research grants OTKA K-081421 and K-109276, and by the STFC Consolidated Grant ST/H00260/1.

Final acknowledgements go to the many observers and astronomers, both amateur and professional, for performing the regular observations of the solar atmosphere and creating the databases of solar indices described in this paper.

References

- J.G. Anet, E.V. Rozanov, S. Muthers, T. Peter, S. BröNnimann, F. Arfeuille, J. Beer, A.I. Shapiro, C.C. Raible, F. Steinhilber, W.K. Schmutz, Impact of a potential 21st century "grand solar minimum" on surface temperatures and stratospheric ozone. *Geophys. Res. Lett.* **40**, 4420–4425 (2013). doi:10.1002/grl.50806
- R. Arlt, R. Leussu, N. Giese, K. Mursula, I.G. Usoskin, Sunspot positions and sizes for 1825–1867 from the observations by Samuel Heinrich Schwabe. *Mon. Not. Roy. Astron. Soc.* **433**, 3165–3172 (2013). doi:10.1093/mnras/stt961
- R. Arlt, N. Weiss, Solar activity in the past and the chaotic behaviour of the dynamo. *Space Science Reviews*, 1–9 (2014). doi:10.1007/s11214-014-0063-5. <http://dx.doi.org/10.1007/s11214-014-0063-5>
- E.H. Avrett, J.M. Fontenla, R. Loeser, Formation of the solar 10830 Å line 1994, pp. 35–47
- H.D. Babcock, The Sun's Polar Magnetic Field. *Astrophys. J.* **130**, 364 (1959). doi:10.1086/146726
- H.D. Babcock, H.W. Babcock, Some New Features of the Solar Spectrum. *Pub. Astron. Soc. Pac.* **46**, 132 (1934). doi:10.1086/124428
- L.A. Balmaceda, S.K. Solanki, N.A. Krivova, S. Foster, A homogeneous database of sunspot areas covering more than 130 years. *Journal of Geophysical Research (Space Physics)* **114**, 7104 (2009). doi:10.1029/2009JA014299
- T. Baranyi, S. Király, H.E. Coffey, Indirect comparison of Debrecen and Greenwich daily suns of sunspot areas. *Mon. Not. Roy. Astron. Soc.* **434**, 1713–1720 (2013). doi:10.1093/mnras/stt1134
- T. Baranyi, L. Gyori, A. Ludmány, H.E. Coffey, Comparison of sunspot area data bases. *Mon. Not. Roy. Astron. Soc.* **323**, 223–230 (2001). doi:10.1046/j.1365-8711.2001.04195.x
- J. Beer, A. Blinov, G. Bonani, H.J. Hofmann, R.C. Finkel, Use of Be-10 in polar ice to trace the 11-year cycle of solar activity. *Nature* **347**, 164–166 (1990). doi:10.1038/347164a0
- A.O. Benz, Flare Observations. *Living Reviews in Solar Physics* **5**, 1 (2008). doi:10.12942/lrsp-2008-1
- L. Bertello, R.K. Ulrich, J.E. Boyden, The Mount Wilson Ca ii K Plage Index Time Series. *Solar Phys.* **264**, 31–44 (2010). doi:10.1007/s11207-010-9570-z
- R. Brajša, S. Pohjolainen, V. Ruždjak, T. Sakurai, S. Urpo, B. Vršnak, H. Wöhl, Helium 10830 Å measurements of the Sun. *Solar Phys.* **163**, 79–91 (1996). doi:10.1007/BF00165457
- D.C. Braun, C. Lindsey, Y. Fan, S.M. Jefferies, Local acoustic diagnostics of the solar interior. *Astrophys. J.* **392**, 739–745 (1992). doi:10.1086/171477
- B. Caccin, I. Ermolli, M. Fofi, A.M. Sambuco, Variations of the Chromospheric Network with the Solar Cycle. *Solar Phys.* **177**, 295–303 (1998). doi:10.1023/A:1004938412420
- W.J. Chaplin, S. Basu, Sounding stellar cycles. *Space Science Reviews* (2014)
- G.A. Chapman, J.J. Dobias, T. Arias, Facular and Sunspot Areas During Solar Cycles 22 and 23. *Astrophys. J.* **728**, 150 (2011). doi:10.1088/0004-637X/728/2/150
- P. Charbonneau, Dynamo Models of the Solar Cycle. *Living Reviews in Solar Physics* **7**, 3 (2010). doi:10.12942/lrsp-2010-3
- P. Charbonneau, A. Choudhury, J. Jang, B. Karak, M. Miesch, Challenges for the solar dynamo. *Space Science Reviews* (2014)
- F. Clette, E. Cliver, L. Svalgaard, The sunspot number in time. *Space Science Reviews* (2014)
- F. Clette, D. Berghmans, P. Vanlommel, R.A.M. Van der Linden, A. Koeckelenbergh, L. Wauters, From the Wolf number to the International Sunspot Index: 25 years of SIDC. *Advances in Space Research* **40**, 919–928 (2007). doi:10.1016/j.asr.2006.12.045
- A.E. Covington, Solar Radio Emission at 10.7 cm, 1947–1968. *JRASC* **63**, 125 (1969)
- S.R. Cranmer, Coronal holes. *Living Reviews in Solar Physics* **6**(3) (2009). doi:10.12942/lrsp-2009-3
- S. Criscuolo, P. Romano, F. Giorgi, F. Zuccarello, Magnetic evolution of superactive regions. Complexity and potentially unstable magnetic discontinuities. *Astron. Astrophys.* **506**, 1429–1436 (2009). doi:10.1051/0004-6361/200912044

- L. Deng, Z. Qi, G. Dun, C. Xu, Phase Relationship between Polar Faculae and Sunspot Numbers Revisited: Wavelet Transform Analyses. *Pub. Astron. Soc. Japan* **65**, 11 (2013). doi:10.1093/pasj/65.1.11
- J.F. Denisse, Microwave solar noise and sunspot. *Astron. J.* **54**, 183 (1949). doi:10.1086/106280
- V. Domingo, I. Ermolli, P. Fox, C. Fröhlich, M. Haberreiter, N. Krivova, G. Kopp, W. Schmutz, S.K. Solanki, H.C. Spruit, Y. Unruh, A. Vögler, Solar Surface Magnetism and Irradiance on Time Scales from Days to the 11-Year Cycle. *Space Sci. Rev.* **145**, 337–380 (2009). doi:10.1007/s11214-009-9562-1
- I. Dorotovič, M. Minarovjech, M. Lorenc, M. Rybanský, Modified Homogeneous Data Set of Coronal Intensities. *Solar Phys.* **289**, 2697–2703 (2014). doi:10.1007/s11207-014-0501-2
- T. Dudok de Wit, S. Bruinsma, K. Shibasaki, Synoptic radio observations as proxies for upper atmosphere modelling. *Journal of Space Weather and Space Climate* **4**(26), 260000 (2014). doi:10.1051/swsc/2014003
- T. Dudok de Wit, M. Kretzschmar, J. Lilensten, T. Woods, Finding the best proxies for the solar UV irradiance. *Geophys. Res. Lett.* **36**, 10107 (2009). doi:10.1029/2009GL037825
- I. Ermolli, S.K. Solanki, A.G. Tlatov, N.A. Krivova, R.K. Ulrich, J. Singh, Comparison Among Ca II K Spectroheliogram Time Series with an Application to Solar Activity Studies. *Astrophys. J.* **698**, 1000–1009 (2009a). doi:10.1088/0004-637X/698/2/1000
- I. Ermolli, E. Marchei, M. Centrone, S. Criscuoli, F. Giorgi, C. Perna, The digitized archive of the Arcetri spectroheliograms. Preliminary results from the analysis of Ca II K images. *Astron. Astrophys.* **499**, 627–632 (2009b). doi:10.1051/0004-6361/200811406
- I. Ermolli, S. Criscuoli, H. Uitenbroek, F. Giorgi, M.P. Rast, S.K. Solanki, Radiative emission of solar features in the Ca II K line: comparison of measurements and models. *Astron. Astrophys.* **523**, 55 (2010). doi:10.1051/0004-6361/201014762
- I. Ermolli, K. Matthes, T. Dudok de Wit, N.A. Krivova, K. Tourpali, M. Weber, Y.C. Unruh, L. Gray, U. Langematz, P. Pilewskie, E. Rozanov, W. Schmutz, A. Shapiro, S.K. Solanki, T.N. Woods, Recent variability of the solar spectral irradiance and its impact on climate modelling. *Atmospheric Chemistry & Physics* **13**, 3945–3977 (2013). doi:10.5194/acp-13-3945-2013
- I. Ermolli, F. Giorgi, P. Romano, F. Zuccarello, S. Criscuoli, M. Stangalini, Fractal and Multifractal Properties of Active Regions as Flare Precursors: A Case Study Based on SOHO/MDI and SDO/HMI Observations. *Solar Phys.* **289**, 2525–2545 (2014). doi:10.1007/s11207-014-0500-3
- Y.P. Fedorenko, O.F. Tyrnov, V.N. Fedorenko, V.L. Dorohov, Model of traveling ionospheric disturbances. *Journal of Space Weather and Space Climate* **3**(26), 30 (2013). doi:10.1051/swsc/2013052
- P. Foukal, L. Bertello, W.C. Livingston, A.A. Pevtsov, J. Singh, A.G. Tlatov, R.K. Ulrich, A Century of Solar Ca II Measurements and Their Implication for Solar UV Driving of Climate. *Solar Phys.* **255**, 229–238 (2009). doi:10.1007/s11207-009-9330-0
- C. Fröhlich, Total Solar Irradiance: What Have We Learned from the Last Three Cycles and the Recent Minimum? *Space Sci. Rev.* **176**, 237–252 (2013). doi:10.1007/s11214-011-9780-1
- G. Galilei, *Istoria e dimostrazioni intorno alle macchie solari* (Accademia dei Lincei, ???, 1613)
- M.K. Georgoulis, Toward an Efficient Prediction of Solar Flares: Which Parameters, and How? *Entropy* **15**, 5022–5052 (2013). doi:10.3390/e15115022
- I. González Hernández, F. Hill, C. Lindsey, Calibration of Seismic Signatures of Active Regions on the Far Side of the Sun. *Astrophys. J.* **669**, 1382–1389 (2007). doi:10.1086/521592
- I. González Hernández, M. Díaz Alfaro, K. Jain, W.K. Tobiska, D.C. Braun, F. Hill, F. Pérez Hernández, A Full-Sun Magnetic Index from Helioseismology Inferences. *Solar Phys.* **289**, 503–514 (2014)
- G.E. Hale, On the Probable Existence of a Magnetic Field in Sun-Spots. *Astrophys. J.* **28**, 315 (1908). doi:10.1086/141602
- G.E. Hale, Sun-spots as Magnets and the Periodic Reversal of their Polarity. *Nature* **113**, 105–112 (1924). doi:10.1038/113105a0
- G.E. Hale, S.B. Nicholson, The Law of Sun-Spot Polarity. *Astrophys. J.* **62**, 270 (1925).

- doi:10.1086/142933
- G.E. Hale, F. Ellerman, S.B. Nicholson, A.H. Joy, The Magnetic Polarity of Sun-Spots. *Astrophys. J.* **49**, 153 (1919). doi:10.1086/142452
- J.C. Hall, Stellar Chromospheric Activity. *Living Reviews in Solar Physics* **5**, 2 (2008). doi:10.12942/lrsp-2008-2
- J.W. Harvey, N.R. Sheeley Jr., A comparison of He II 304 Å and He I 10,830 Å spectroheliograms. *Solar Phys.* **54**, 343–351 (1977). doi:10.1007/BF00159924
- K.L. Harvey, The relationship between coronal bright points as seen in He I Lambda 10830 and the evolution of the photospheric network magnetic fields. *Australian Journal of Physics* **38**, 875–883 (1985)
- K.L. Harvey, The Cyclic Behavior of Solar Activity, in *The Solar Cycle*, ed. by K.L. Harvey Astronomical Society of the Pacific Conference Series, vol. 27, 1992, p. 335
- K.L. Harvey, F. Recely, Polar Coronal Holes During Cycles 22 and 23. *Solar Phys.* **211**, 31–52 (2002). doi:10.1023/A:1022469023581
- D.H. Hathaway, The Solar Cycle. *Living Reviews in Solar Physics* **7**, 1 (2010). doi:10.12942/lrsp-2010-1
- D.H. Hathaway, R.M. Wilson, What the Sunspot Record Tells Us About Space Climate. *Solar Phys.* **224**, 5–19 (2004). doi:10.1007/s11207-005-3996-8
- D.F. Heath, B.M. Schlesinger, The Mg 280-nm doublet as a monitor of changes in solar ultraviolet irradiance. *J. Geophys. Res.* **91**, 8672–8682 (1986). doi:10.1029/JD091iD08p08672
- C.J. Henney, W.A. Toussaint, S.M. White, C.N. Arge, Forecasting F_{10.7} with solar magnetic flux transport modeling. *Space Weather* **10**, 2011 (2012). doi:10.1029/2011SW000748
- D.V. Hoyt, K.H. Schatten, How Well Was the Sun Observed during the Maunder Minimum? *Solar Phys.* **165**, 181–192 (1996). doi:10.1007/BF00149097
- D.V. Hoyt, K.H. Schatten, Group Sunspot Numbers: A New Solar Activity Reconstruction. *Solar Phys.* **179**, 189–219 (1998a). doi:10.1023/A:1005007527816
- D.V. Hoyt, K.H. Schatten, Group Sunspot Numbers: A New Solar Activity Reconstruction. *Solar Phys.* **181**, 491–512 (1998b). doi:10.1023/A:1005056326158
- H. Hudson, L. Fletcher, J. McTiernan, Cycle 23 Variation in Solar Flare Productivity. *Solar Phys.* **289**, 1341–1347 (2014a). doi:10.1007/s11207-013-0384-7
- H. Hudson, L. Svalgaard, E. Cliver, Solar sector structure. *Space Science Reviews* (2014b)
- H.S. Hudson, S. Silva, M. Woodard, R.C. Willson, The effects of sunspots on solar irradiance. *Solar Phys.* **76**, 211–219 (1982). doi:10.1007/BF00170984
- K. Jain, S.S. Hasan, Modulation in the solar irradiance due to surface magnetism during cycles 21, 22 and 23. *Astron. Astrophys.* **425**, 301–307 (2004). doi:10.1051/0004-6361:20047102
- J. Jiang, R.H. Cameron, D. Schmitt, M. Schüssler, The solar magnetic field since 1700. II. Physical reconstruction of total, polar and open flux. *Astron. Astrophys.* **528**, 83 (2011). doi:10.1051/0004-6361/201016168
- A. Kerdran, J.-M. Delouis, The Nançay Radioheliograph, in *Coronal Physics from Radio and Space Observations*, ed. by G. Trottet Lecture Notes in Physics, Berlin Springer Verlag, vol. 483, 1997, p. 192. doi:10.1007/BFb0106458
- C. Kiess, R. Rezaei, W. Schmidt, Properties of sunspot umbrae observed in Cycle 24. ArXiv e-prints (2014)
- J. Kleczek, Ionospheric Disturbances and Flares in the 11 - years cycle. *Bulletin of the Astronomical Institutes of Czechoslovakia* **3**, 52 (1952)
- N.A. Krivova, L.E.A. Vieira, S.K. Solanki, Reconstruction of solar spectral irradiance since the Maunder minimum. *Journal of Geophysical Research (Space Physics)* **115**, 12112 (2010). doi:10.1029/2010JA015431
- M.R. Kundu, Solar Active Regions at Millimeter Wavelengths. *Solar Phys.* **13**, 348–356 (1970). doi:10.1007/BF00153556
- I. Kutiev, I. Tsagouri, L. Perrone, D. Pancheva, P. Mukhtarov, A. Mikhailov, J. Lastovicka, N. Jakowski, D. Buresova, E. Blanch, B. Andonov, D. Altadill, S. Magdaleno, M. Parisi, J. Miquel Torta, Solar activity impact on the Earth's upper atmosphere. *Journal of Space Weather and Space Climate* **3**(26), 6 (2013). doi:10.1051/swsc/2013028
- A. Lagg, Recent advances in measuring chromospheric magnetic fields in the He I 10830 Å line. *Advances in Space Research* **39**, 1734–1740 (2007). doi:10.1016/j.asr.2007.03.091

- J.L. Lean, T.N. Woods, F.G. Eparvier, R.R. Meier, D.J. Strickland, J.T. Correira, J.S. Evans, Solar extreme ultraviolet irradiance: Present, past, and future. *Journal of Geophysical Research (Space Physics)* **116**, 1102 (2011). doi:10.1029/2010JA015901
- J. Leenaarts, M. Carlsson, L. Rouppe van der Voort, The Formation of the H α Line in the Solar Chromosphere. *Astrophys. J.* **749**, 136 (2012). doi:10.1088/0004-637X/749/2/136
- J. Leenaarts, T.M.D. Pereira, M. Carlsson, H. Uitenbroek, B. De Pontieu, The Formation of IRIS Diagnostics. II. The Formation of the Mg II h and k Lines in the Solar Atmosphere. *Astrophys. J.* **772**, 90 (2013). doi:10.1088/0004-637X/772/2/90
- L. Lefevre, F. Clette, Survey and Merging of Sunspot Catalogs. *Solar Phys.* **289**, 545–561 (2014). doi:10.1007/s11207-012-0184-5
- D.K. Lepshokov, A.G. Tlatov, V.V. Vasil'eva, Reconstruction of sunspot characteristics for 1853–1879. *Geomagnetism and Aeronomy* **52**, 843–848 (2012). doi:10.1134/S0016793212070109
- R. Leussu, I.G. Usoskin, R. Arlt, K. Mursula, Inconsistency of the Wolf sunspot number series around 1848. *Astron. Astrophys.* **559**, 28 (2013). doi:10.1051/0004-6361/201322373
- K.J. Li, P.X. Gao, L.S. Zhan, Synchronization of Sunspot Numbers and Sunspot Areas. *Solar Phys.* **255**, 289–300 (2009). doi:10.1007/s11207-009-9328-7
- C. Lindsey, D.C. Braun, Helioseismic Holography. *Astrophys. J.* **485**, 895 (1997). doi:10.1086/304445
- Y. Liu, J.T. Hoeksema, P.H. Scherrer, J. Schou, S. Couvidat, R.I. Bush, T.L. Duvall, K. Hayashi, X. Sun, X. Zhao, Comparison of Line-of-Sight Magnetograms Taken by the Solar Dynamics Observatory/Helioseismic and Magnetic Imager and Solar and Heliospheric Observatory/Michelson Doppler Imager. *Solar Phys.* **279**, 295–316 (2012). doi:10.1007/s11207-012-9976-x
- M. Lockwood, Reconstruction and prediction of variations in the open solar magnetic flux and interplanetary conditions. *Living Reviews in Solar Physics* **10**(4) (2013). doi:10.12942/lrsp-2013-4. <http://www.livingreviews.org/lrsp-2013-4>
- J.N. Lockyer, Supplementary Note on a Spectrum of a Solar Prominence. *Royal Society of London Proceedings Series I* **17**, 128 (1868)
- V.I. Makarov, A.G. Tlatov, The Large-Scale Solar Magnetic Field and 11-Year Activity Cycles. *Astronomy Reports* **44**, 759–764 (2000). doi:10.1134/1.1320502
- V.I. Makarov, A.G. Tlatov, D.K. Callebaut, V.N. Obridko, B.D. Shelting, Large-Scale Magnetic Field and Sunspot Cycles. *Solar Phys.* **198**, 409–421 (2001). doi:10.1023/A:1005249531228
- T. Maruyama, Solar proxies pertaining to empirical ionospheric total electron content models. *Journal of Geophysical Research (Space Physics)* **115**, 4306 (2010). doi:10.1029/2009JA014890
- K. Matthes, K. Kodera, R.R. Garcia, Y. Kuroda, D.R. Marsh, K. Labitzke, The importance of time-varying forcing for QBO modulation of the atmospheric 11 year solar cycle signal. *Journal of Geophysical Research (Atmospheres)* **118**, 4435–4447 (2013). doi:10.1002/jgrd.50424
- E.W. Maunder, Note on the distribution of sun-spots in heliographic latitude, 1874–1902. *Mon. Not. Roy. Astron. Soc.* **64**, 747–761 (1904)
- B. Mendoza, V.M. Velasco-Herrera, On Mid-Term Periodicities in Sunspot Groups and Flare Index. *Solar Phys.* **271**, 169–182 (2011). doi:10.1007/s11207-011-9802-x
- B. Mendoza, V.M. Mendoza, R. Garduño, J. Adem, Modelling the Northern Hemisphere temperature for solar cycles 24 and 25. *Journal of Atmospheric and Solar-Terrestrial Physics* **72**, 1122–1128 (2010). doi:10.1016/j.jastp.2010.05.018
- M. Minarovjech, V. Rušin, M. Saniga, The green corona database and the coronal index of solar activity. *Contributions of the Astronomical Observatory Skalnaté Pleso* **41**, 137–141 (2011)
- Z. Mouradian, Synoptic Data Findings, in *Synoptic Solar Physics*, ed. by K.S. Balasubramaniam, J. Harvey, D. Rabin *Astronomical Society of the Pacific Conference Series*, vol. 140, 1998, p. 181
- A. Muñoz-Jaramillo, N.R. Sheeley, J. Zhang, E.E. DeLuca, Calibrating 100 Years of Polar Faculae Measurements: Implications for the Evolution of the Heliospheric Magnetic Field. *Astrophys. J.* **753**, 146 (2012). doi:10.1088/0004-637X/753/2/146
- A. Norton, P. Charbonneau, Observed solar N-S asymmetry in relation to dynamo modeling.

- Space Science Reviews (2014)
- S. Oberländer, U. Langematz, K. Matthes, M. Kunze, A. Kubin, J. Harder, N.A. Krivova, S.K. Solanki, J. Paganan, M. Weber, The influence of spectral solar irradiance data on stratospheric heating rates during the 11 year solar cycle. *Geophys. Res. Lett.* **39**, 1801 (2012). doi:10.1029/2011GL049539
- K. Oláh, Z. Kolláth, T. Granzer, K.G. Strassmeier, A.F. Lanza, S. Järvinen, H. Korhonen, S.L. Baliunas, W. Soon, S. Messina, G. Cutispoto, Multiple and changing cycles of active stars. II. Results. *Astron. Astrophys.* **501**, 703–713 (2009). doi:10.1051/0004-6361/200811304
- M.J. Owens, R.J. Forsyth, The heliospheric magnetic field. Living Reviews in Solar Physics **10**(5) (2013). doi:10.12942/lrsp-2013-5. <http://www.livingreviews.org/lrsp-2013-5>
- A. Özgüç, T. Ataç, J. Rybák, Temporal variability of the flare index (1966-2001). *Solar Phys.* **214**, 375–396 (2003). doi:10.1023/A:1024225802080
- J. Paganan, M. Weber, J. Burrows, Solar Variability from 240 to 1750 nm in Terms of Faculae Brightening and Sunspot Darkening from SCIAMACHY. *Astrophys. J.* **700**, 1884–1895 (2009a). doi:10.1088/0004-637X/700/2/1884
- J. Paganan, M. Weber, J. Burrows, Solar Variability from 240 to 1750 nm in Terms of Faculae Brightening and Sunspot Darkening from SCIAMACHY. *Astrophys. J.* **700**, 1884–1895 (2009b). doi:10.1088/0004-637X/700/2/1884
- W.D. Pesnell, Solar Cycle Predictions (Invited Review). *Solar Phys.* **281**, 507–532 (2012). doi:10.1007/s11207-012-9997-5
- C. Petrick, K. Matthes, H. Dobsław, M. Thomas, Impact of the solar cycle and the QBO on the atmosphere and the ocean. *Journal of Geophysical Research (Atmospheres)* **117**, 17111 (2012). doi:10.1029/2011JD017390
- G.J.D. Petrie, Solar Magnetic Activity Cycles, Coronal Potential Field Models and Eruption Rates. *Astrophys. J.* **768**, 162 (2013). doi:10.1088/0004-637X/768/2/162
- G.J.D. Petrie, K. Petrovay, K. Schatten, Solar polar fields and the 22-year activity cycle: Observations and models. *Space Science Reviews*, 1–33 (2014). doi:10.1007/s11214-014-0064-4. <http://dx.doi.org/10.1007/s11214-014-0064-4>
- A.A. Pevtsov, L. Bertello, H. Uitenbroek, On Possible Variations of Basal Ca II K Chromospheric Line Profiles with the Solar Cycle. *Astrophys. J.* **767**, 56 (2013). doi:10.1088/0004-637X/767/1/56
- M.S. Potgieter, Solar modulation of cosmic rays. Living Reviews in Solar Physics **10**(3) (2013). doi:10.12942/lrsp-2013-3
- D.G. Preminger, S.R. Walton, Modeling Solar Spectral Irradiance and Total Magnetic Flux Using Sunspot Areas. *Solar Phys.* **235**, 387–405 (2006). doi:10.1007/s11207-006-0044-2
- D.G. Preminger, S.R. Walton, From Sunspot Area to Solar Variability: A Linear Transformation. *Solar Phys.* **240**, 17–23 (2007). doi:10.1007/s11207-007-0335-2
- M. Priyal, J. Singh, B. Ravindra, T.G. Priya, K. Amareswari, Long Term Variations in Chromospheric Features from Ca-K Images at Kodaikanal. *Solar Phys.* **289**, 137–152 (2014). doi:10.1007/s11207-013-0315-7
- T. Pulkkinen, Space Weather: Terrestrial Perspective. Living Reviews in Solar Physics **4**, 1 (2007). doi:10.12942/lrsp-2007-1
- T.I. Pulkkinen, M. Palmroth, E.I. Tanskanen, N.Y. Ganushkina, M.A. Shukhtina, N.P. Dmitrieva, Solar wind magnetosphere coupling: A review of recent results. *Journal of Atmospheric and Solar-Terrestrial Physics* **69**, 256–264 (2007). doi:
- A. Reiners, Observations of Cool-Star Magnetic Fields. Living Reviews in Solar Physics **9**, 1 (2012). doi:10.12942/lrsp-2012-1
- P. Riley, R. Lionello, J.A. Linker, Z. Mikic, J. Luhmann, J. Wijaya, Global MHD Modeling of the Solar Corona and Inner Heliosphere for the Whole Heliosphere Interval. *Solar Phys.* **274**, 361–377 (2011). doi:10.1007/s11207-010-9698-x
- P. Riley, M. Ben-Nun, J.A. Linker, Z. Mikic, L. Svalgaard, J. Harvey, L. Bertello, T. Hoeksema, Y. Liu, R. Ulrich, A Multi-Observatory Inter-Comparison of Line-of-Sight Synoptic Solar Magnetograms. *Solar Phys.* **289**, 769–792 (2014). doi:10.1007/s11207-013-0353-1
- R.J. Rutten, Observing the Solar Chromosphere, in *The Physics of Chromospheric Plasmas*, ed. by P. Heinzel, I. Dorotovič, R.J. Rutten. Astronomical Society of the Pacific Conference Series, vol. 368, 2007, p. 27

- V. Rušin, M. Rybansky, The Green Corona and Magnetic Fields. *Solar Phys.* **207**, 47–61 (2002). doi:10.1023/A:1015587719072
- M. Rybanský, V. Rušin, M. Minarovjech, Coronal index of solar activity - Solar-terrestrial research. *Space Sci. Rev.* **95**, 227–234 (2001)
- M. Rybanský, V. Rušin, M. Minarovjech, L. Klocok, E.W. Cliver, Reexamination of the coronal index of solar activity. *Journal of Geophysical Research (Space Physics)* **110**, 8106 (2005). doi:10.1029/2005JA011146
- J.D. Scargle, S.L. Keil, S.P. Worden, Solar Cycle Variability and Surface Differential Rotation from Ca II K-line Time Series Data. *Astrophys. J.* **771**, 33 (2013). doi:10.1088/0004-637X/771/1/33
- C. Scheiner, *Rosa Ursina Sive Sol* 1626–1630
- B. Schmieder, V. Archontis, M. Schuessler, E. Pariat, Magnetic flux emergence. *Space Science Reviews* (2014)
- C.J. Schrijver, J. Cote, C. Zwaan, S.H. Saar, Relations between the photospheric magnetic field and the emission from the outer atmospheres of cool stars. I - The solar CA II K line core emission. *Astrophys. J.* **337**, 964–976 (1989). doi:10.1086/167168
- M. Schwabe, Die Sonne. Von Herrn Hofrath Schwabe. *Astronomische Nachrichten* **20**, 283 (1843). doi:10.1002/asna.18430201706
- C.J. Scott, R.G. Harrison, M.J. Owens, M. Lockwood, L. Barnard, Evidence for solar wind modulation of lightning. *Environmental Research Letters* **9**(5), 055004 (2014). doi:10.1088/1748-9326/9/5/055004
- N.R. Sheeley Jr., A Century of Polar Faculae Variations. *Astrophys. J.* **680**, 1553–1559 (2008). doi:10.1086/588251
- N.R. Sheeley Jr., T.J. Cooper, J.R.L. Anderson, Carrington Maps of Ca II K-line Emission for the Years 1915–1985. *Astrophys. J.* **730**, 51 (2011). doi:10.1088/0004-637X/730/1/51
- K. Shibasaki, C.E. Alissandrakis, S. Pohjolainen, Radio Emission of the Quiet Sun and Active Regions (Invited Review). *Solar Phys.* **273**, 309–337 (2011). doi:10.1007/s11207-011-9788-4
- K. Shibata, T. Magara, Solar Flares: Magnetohydrodynamic Processes. *Living Reviews in Solar Physics* **8**, 6 (2011). doi:10.12942/lrsp-2011-6
- S. Solanki, N. Krivova, Faculae and Plague. *Landolt Börnstein*, 4124 (2009). doi:
- S.K. Solanki, B. Inhester, M. Schüssler, The solar magnetic field. *Reports on Progress in Physics* **69**, 563–668 (2006). doi:10.1088/0034-4885/69/3/R02
- S.K. Solanki, N.A. Krivova, J.D. Haigh, Solar Irradiance Variability and Climate. *Annual Rev. Astron. Astrophys.* **51**, 311–351 (2013). doi:10.1146/annurev-astro-082812-141007
- J.O. Stenflo, Solar magnetic fields. *Journal of Astrophysics and Astronomy* **29**, 19–28 (2008). doi:10.1007/s12036-008-0003-4
- J.O. Stenflo, Solar magnetic fields as revealed by Stokes polarimetry. *Astron. Astrophys. Rev.* **21**, 66 (2013). doi:10.1007/s00159-013-0066-3
- M. Stuiver, P.D. Quay, Changes in atmospheric Carbon-14 attributed to a variable sun. *Science* **207**, 11–19 (1980). doi:10.1126/science.207.4426.11
- W.T. Sullivan, *The early years of radio astronomy - Reflections fifty years after Jansky's discovery* 1984
- L. Svalgaard, What geomagnetism can tell us about the solar cycle? *Space Science Reviews* (2014)
- L. Svalgaard, H.S. Hudson, The Solar Microwave Flux and the Sunspot Number, in *SOHO-23: Understanding a Peculiar Solar Minimum*, ed. by S.R. Cranmer, J.T. Hoeksema, J.L. Kohl *Astronomical Society of the Pacific Conference Series*, vol. 428, 2010, p. 325
- H. Tanaka, J.P. Castelli, A.E. Covington, A. Krüger, T.L. Landecker, A. Tlamicha, Absolute Calibration of Solar Radio Flux Density in the Microwave Region. *Solar Phys.* **29**, 243–262 (1973). doi:10.1007/BF00153452
- K.F. Tapping, The 10.7 cm solar radio flux ($F_{10.7}$). *Space Weather* **11**, 394–406 (2013). doi:10.1002/swe.20064
- K.F. Tapping, J.J. Valdés, Did the Sun Change Its Behaviour During the Decline of Cycle 23 and Into Cycle 24? *Solar Phys.* **272**, 337–350 (2011). doi:10.1007/s11207-011-9827-1
- M. Temmer, A. Veronig, A. Hanslmeier, Hemispheric Sunspot Numbers R_n and R_s : Catalogue and N-S asymmetry analysis. *Astron. Astrophys.* **390**, 707–715 (2002).

- doi:10.1051/0004-6361:20020758
- M. Temmer, J. Rybák, P. Bendík, A. Veronig, F. Vogler, W. Otruba, W. Pötzi, A. Hanslmeier, Hemispheric sunspot numbers $\{R_n\}$ and $\{R_s\}$ from 1945-2004: catalogue and N-S asymmetry analysis for solar cycles 18-23. *Astron. Astrophys.* **447**, 735–743 (2006). doi:10.1051/0004-6361:20054060
- G. Thuillier, S.M.L. Melo, J. Lean, N.A. Krivova, C. Bolduc, V.I. Fomichev, P. Charbonneau, A.I. Shapiro, W. Schmutz, D. Bolsée, Analysis of Different Solar Spectral Irradiance Reconstructions and Their Impact on Solar Heating Rates. *Solar Phys.* **289**, 1115–1142 (2014). doi:10.1007/s11207-013-0381-x
- H. Uitenbroek, Operator perturbation method for multi-level line transfer with partial redistribution. *Astron. Astrophys.* **213**, 360–370 (1989)
- I.G. Usoskin, A History of Solar Activity over Millennia. *Living Reviews in Solar Physics* **10**, 1 (2013). doi:10.12942/lrsp-2013-1
- I. Usoskin, G. Bazilevskaya, E. Cliver, G. Kovaltsov, Solar cycle in the heliosphere and cosmic rays. *Space Science Reviews* (2014)
- H. van Loon, J. Brown, R.F. Milliff, Trends in sunspots and North Atlantic sea level pressure. *Journal of Geophysical Research (Atmospheres)* **117**, 7106 (2012). doi:10.1029/2012JD017502
- J.M. Vaquero, R.M. Trigo, Revised Group Sunspot Number Values for 1640, 1652, and 1741. *Solar Phys.* **289**, 803–808 (2014). doi:10.1007/s11207-013-0360-2
- J.M. Vaquero, R.M. Trigo, M.C. Gallego, A Simple Method to Check the Reliability of Annual Sunspot Number in the Historical Period 1610 - 1847. *Solar Phys.* **277**, 389–395 (2012). doi:10.1007/s11207-011-9901-8
- V.V. Vasil'Eva, V.I. Makarov, A.G. Tlatov, Rotation Cycles of the Sector Structure of the Solar Magnetic Field and Its Activity. *Astronomy Letters* **28**, 199–205 (2002). doi:10.1134/1.1458351
- I.I. Virtanen, K. Mursula, North-South Asymmetric Solar Cycle Evolution: Signatures in the Photosphere and Consequences in the Corona. *Astrophys. J.* **781**, 99 (2014). doi:10.1088/0004-637X/781/2/99
- Y.-M. Wang, Solar cycle variation of the sun's low-order magnetic multipoles: Heliospheric consequences. *Space Science Reviews*, 1–21 (2014). doi:10.1007/s11214-014-0051-9. <http://dx.doi.org/10.1007/s11214-014-0051-9>
- D.M. Willis, R. Henwood, M.N. Wild, H.E. Coffey, W.F. Denig, E.H. Erwin, D.V. Hoyt, The Greenwich Photo-heliographic Results (1874 - 1976): Procedures for Checking and Correcting the Sunspot Digital Datasets. *Solar Phys.* **288**, 141–156 (2013a). doi:10.1007/s11207-013-0312-x
- D.M. Willis, H.E. Coffey, R. Henwood, E.H. Erwin, D.V. Hoyt, M.N. Wild, W.F. Denig, The Greenwich Photo-heliographic Results (1874 - 1976): Summary of the Observations, Applications, Datasets, Definitions and Errors. *Solar Phys.* **288**, 117–139 (2013b). doi:10.1007/s11207-013-0311-y
- R.C. Willson, S. Gulkis, M. Janssen, H.S. Hudson, G.A. Chapman, Observations of solar irradiance variability. *Science* **211**, 700–702 (1981). doi:10.1126/science.211.4483.700
- K.L. Yeo, N.A. Krivova, S.K. Solanki, Solar cycle variation in solar irradiance. *Space Science Reviews*, 1–31 (2014). doi:10.1007/s11214-014-0061-7. <http://dx.doi.org/10.1007/s11214-014-0061-7>